

# NMSSM Explanations of the Galactic Gamma Ray Excess and Promising LHC Searches

---

Jun Guo,<sup>a</sup> Jinmian Li,<sup>b</sup> Tianjun Li<sup>a,c</sup> and Anthony G. Williams<sup>b</sup>

<sup>a</sup>*State Key Laboratory of Theoretical Physics, Institute of Theoretical Physics, Chinese Academy of Sciences, Beijing 100190, P. R. China*

<sup>b</sup>*ARC Centre of Excellence for Particle Physics at the Terascale, School of Chemistry and Physics, University of Adelaide, Adelaide, SA 5005, Australia*

<sup>c</sup>*School of Physical Electronics, University of Electronic Science and Technology of China, Chengdu 610054, P. R. China*

*E-mail:* [hustgj@itp.ac.cn](mailto:hustgj@itp.ac.cn), [jinmian.li@adelaide.ac.au](mailto:jinmian.li@adelaide.ac.au), [tli@itp.ac.cn](mailto:tli@itp.ac.cn),  
[anthony.williams@adelaide.edu.au](mailto:anthony.williams@adelaide.edu.au)

**ABSTRACT:** To explain the Galactic Center Gamma-ray Excess (GCGE), we consider three possible scenarios in the Next-to-Minimal Supersymmetric Standard Model (NMSSM) with  $Z_3$  symmetry: (i) The  $s$ -channel  $A_1$  resonant annihilation scenario; (ii) The hidden sector dark matter scenario; (iii) The sbottom and stau coannihilation scenarios. We show that the first scenario is the most favourable one, and we study its LHC discovery potential via four signatures. We find that the most sensitive signals are provided by the Higgsino-like chargino and neutralino pair productions with their subsequent decays into  $W$  bosons,  $Z$  bosons, and dark matter. The majority of the interesting model space can be probed at the Large Hadron Collider with a centre-of-mass energy of 14 TeV and the integrated luminosity  $1000 \text{ fb}^{-1}$ .

**KEYWORDS:** NMSSM, Galactic Center Gamma-ray Excess, Dark Matter, LHC

---

## Contents

<b>1</b>	<b>Introduction</b>	<b>1</b>
<b>2</b>	<b>Dark Matter Annihilation and GCGE</b>	<b>3</b>
<b>3</b>	<b>GCGE in the NMSSM</b>	<b>4</b>
3.1	<i>s</i> -Channel $A_1$ Resonant Annihilation	5
3.2	Hidden Sector Dark Matter in the NMSSM	12
3.3	Sbottom and Stau Coannihilation	15
<b>4</b>	<b>Discovery Potential at the LHC</b>	<b>16</b>
4.1	Dark Matter Production Versus Mono-jet	17
4.2	Searching the Di-Higgs Final State	17
4.3	Extrapolating the ATLAS Electroweakino Searches at 14 TeV LHC	19
4.3.1	$WH$ Final States	19
4.3.2	$WZ$ Final States	20
<b>5</b>	<b>Conclusion</b>	<b>22</b>
	<b>Appendix A Neutralino and Higgs Mass Matrices</b>	<b>23</b>

---

## 1 Introduction

The most convincing evidence of the existence of Dark Matter (DM) is from the gravitational effects, for example, the rotation curves of spiral galaxies and studies of mass distributions through gravitational lensing. However, the DM particle(s) and its (their) non-gravitational interactions remain unknown. Especially, the absence of convincing signals in spin independent DM direct detection experiments [1, 2] already imposed very stringent constraints on the upper limits for the DM couplings to the Standard Model (SM) particles.

DM can also be probed through indirect signals by producing anomalies in gamma ray, anti-proton, electron, and positron spectra, etc. A recent analysis of the Fermi Gamma-Ray Space Telescope data [3], has shown an significant excess of gamma rays from the Galactic Center (GC). This GC Gamma-Ray Excess (GCGE) in the range of  $\sim [1, 3]$  GeV can be fitted very well by a 31-40 GeV DM annihilating into  $b\bar{b}$  with an annihilation cross section of  $\sigma v = (1.4 \sim 2.0) \times 10^{-26} \text{ cm}^3/\text{s}$ , or a 7-10 GeV DM particle annihilating into  $\tau\bar{\tau}$  with similar cross section. How to explain the GCGE has been studied extensively in both model-dependent and model-independent ways [4–28].

It is well-known that supersymmetry (SUSY) provides a natural solution to the gauge hierarchy problem in the SM. In the supersymmetric SMs (SSMs), gauge coupling unification can be realized, which strongly indicates the Grand Unified Theory (GUT). And if  $R$ -parity is conserved, the lightest supersymmetric particle (LSP) such as neutralino is a good cold DM candidate. In short, SUSY is one of the most promising candidates for new physics beyond the SM. However, the Minimal SSM (MSSM) is challenged by the discovery of the 125 GeV Higgs boson [29, 30] due to the so-called little hierarchy problem about the fine tuning on electroweak scale. In the Next-to-MSSM (NMSSM) [31], the SM-like Higgs boson mass can be lifted by both tree level coupling and the mixing with a lighter singlet [32–42]. Thus, one can naturally obtain a relatively heavy Higgs boson. What’s more, the NMSSM has the advantages by solving the  $\mu$  problem in the MSSM and providing a potential explanation of di-photon excess in Higgs decay. However, with regard to the latter, recent results from the ATLAS and CMS Collaborations suggest that there is no statistical significance to the previously reported di-photon excess [43, 44]. In this paper, we will demonstrate another merit of the NMSSM, which explains the GCGE elegantly through a light singlet-like CP-odd Higgs.

To explore the possible explanations for the GCGE, we consider three scenarios in the NMSSM with a  $Z_3$  discrete symmetry

- (i)  $s$ -channel  $A_1$  resonant annihilation – In this scenario, the final state is mainly  $b\bar{b}$  because the  $b$  quark has a relatively larger Yukawa coupling and the singlet-like CP-odd Higgs boson has mass  $m_{A_1} \simeq 2m_{\text{DM}}$ . We find that DM is required to have small Higgsino component in order to realize the correct DM relic density while evade the current direct detection bounds;
- (ii) Hidden sector dark matter – In this scenario, the DM particles, which do not have any couplings directly to the SM particles, can annihilate into two singlet-like Higgs bosons, which subsequently decay into the SM particles typically dominated by  $b\bar{b}$ . However, there is a tension between the large DM-singlet coupling and a decoupled Higgsino. As a result, the annihilation cross section has an upper bound from the DM direct detections, which is about a factor 2 smaller than the needed value.
- (iii) Sbottom and stau co-annihilations - In this scenario, DM is annihilating through the  $t$ -channel sbottom/stau process. As we will discuss below, the sbottom co-annihilation scenario is excluded by the DM direct detection while the stau co-annihilation scenario with  $m_{\tilde{\tau}} \sim 10$  GeV is in conflict with the  $Z$  boson invisible decays.

Meanwhile, the CERN Large Hadron Collider (LHC) is vigorously continuing its searches for evidence of SUSY. The current searches have excluded electroweakinos with masses below  $\sim 700$  GeV [45]. The next run of LHC at a centre-of-mass energy of 14 TeV will start next year. If SUSY was not found, it will provide even more stringent lower mass bounds on all SUSY particles. Thus, how to probe our above NMSSM scenario at the 14 TeV LHC is an interesting question. On the one hand, DM is likely to have relatively large annihilation cross section to the SM particles in order to reproduce both the correct DM relic density and the GCGE. The inverse process may help to produce significant numbers

of DM pairs at the LHC if the DM mass is not too high. On the other hand, the GCGE scenarios in the NMSSM generically have light Higgsinos as well. So, probing the existence of a relatively light Higgsino can become a smoking gun of an explanation of the GCGE in the NMSSM. We conclude that it will be difficult to search for the direct DM pair productions with mono-jet signature, whereas most of the viable parameter space is discoverable at 14 TeV LHC with  $1000 \text{ fb}^{-1}$  of data by searching for  $WZ + \text{DMs}$  final states decaying from Higgsinos.

This paper is organised as follows. In Section 2, based on the analysis in Ref. [3], we briefly introduce the gamma ray flux measurement at the galactic centre. We study all three possible scenarios in the NMSSM in Section 3. In Section 4, we discuss some potential signatures and their discovery potential at the LHC. In particular, we investigate the required data sample necessary to fully explore the viable parameter space. Finally, we summarise and present our conclusion in Section 5.

## 2 Dark Matter Annihilation and GCGE

The indirect detection, which mainly focuses on DM annihilation final states, is an important method to search for the DM. Galactic centre has relatively large DM number density due to gravity effects, and then it is one of the most promising place for dark matter indirect detection. The searches for gamma ray has much more advantages over the other indirect searches for anti-proton, positron, and electron, as gamma rays can neither deflected by magnetic field nor lost energy during their propagation.

The gamma-ray flux, which was produced from DM annihilation and then detected near the Earth, is given by

$$\frac{d\Phi}{dE_\gamma} = \frac{1}{4\pi} \frac{\langle\sigma v\rangle}{2m_{DM}^2} \frac{dN_\gamma}{dE_\gamma} \int_{\Delta\Omega} \langle J \rangle d\Omega' , \quad (2.1)$$

where

$$\langle J \rangle = \int_{l.o.s} \rho^2(\mathbf{r}) dl \quad (2.2)$$

is called J-factor which encapsulates the dark matter distribution integrated over a solid angle  $\Delta\Omega$ , and  $dN_\gamma/dE_\gamma$  is the gamma-ray spectrum which mainly depends on the properties of the annihilation final states and their kinematical features. Here,  $\rho(\mathbf{R})$  is the dark matter density distribution of a given dark matter halo profile.

The Milky Way's dark matter density distribution is assumed to be approximately spherically symmetric, which can be simplified as a function of distance from the Galactic Center. Usually, the NFW (Einasto and Navarro, Frenk and White) profile [46, 47], which provides good fits to dark matter numerical simulations, is given by

$$\rho(r) = \rho_s \left(\frac{r}{r_s}\right)^{-\gamma} \left[1 + \left(\frac{r}{r_s}\right)\right]^{\gamma-3} \quad (2.3)$$

where  $\rho_s$  is the dark matter density around sun (the distance from sun to the Galactic Center is 8.5 kpc), *i.e.*,  $\rho_s = 0.3 \text{ GeV cm}^{-3}$ . In the analysis of Ref. [3], the scale value is

adopted to be  $r_s = 20$  kpc. For those DM indirect detections which focus on the Galactic Center, the uncertainty of  $\rho^2(\mathbf{r})$  is large at small radius and may even become divergent close to the center. The canonical NFW value of  $\gamma$  is 1, while  $\gamma = 1.2$  is chosen in Ref [3] to get a best fit.

The J-factor can be rewritten as follows

$$J = \int db \int dl \int ds \cos b \rho(r)^2, \quad (2.4)$$

in which  $r = (s^2 + r_s^2 - 2sr_s \cos l \cos b)^{1/2}$  is the Galactocentric distance, and  $(l, b)$  are respectively the longitude and latitude angles. Ref. [3] considered the gamma spectra within a  $5^\circ \times 5^\circ$  region around Galactic Center. And  $s$  is the line of sight distance which has to be integrated.

The last and most important factor-annihilation cross section  $\langle\sigma v\rangle$ , which can affect both indirect detection and DM relic density, is a model dependent variable. The relic density approximately is

$$\Omega h^2 = \frac{m_\chi n_\chi}{\rho_c} \simeq \frac{3 \times 10^{-27} \text{cm}^3 \text{s}^{-1}}{\langle\sigma v\rangle}. \quad (2.5)$$

At the freeze-out  $v \sim 0.1$ , one usually needs an annihilation cross section around 1 pb to produce the correct relic density  $\Omega h^2 \simeq 0.1$  [48]. The analysis of Ref [3] showed that if the DM annihilation only into  $b\bar{b}$  final states with  $v \sim 10^{-3}$ , one would need  $\langle\sigma v\rangle \simeq 2.2 \times 10^{-26} \text{cm}^3 \text{s}^{-1}$  to produce the observed Gamma Ray Excess. Surprisingly, such annihilation cross section can almost lead to the observed relic density. Because the annihilation cross section can be written as  $\langle\sigma v\rangle = a + bv^2$ , when  $v$  is small, we may conclude that the  $\langle\sigma v\rangle$  should be dominated by the  $s$ -wave annihilation.

### 3 GCGE in the NMSSM

In this Section, we will apply the Galactic Center Gamma-ray Excess to a phenomenological NMSSM with  $Z_3$  discrete symmetry. The corresponding superpotential is [31]

$$W_{\text{NMSSM}} = h_u \hat{H}_u \hat{Q} \hat{U}_R^c + h_d \hat{H}_d \hat{Q} \hat{D}_R^c + h_e \hat{H}_d \hat{L} \hat{E}_R^c + \lambda \hat{S} \hat{H}_u \hat{H}_d + \frac{\kappa}{3} \hat{S}^3, \quad (3.1)$$

where  $\hat{Q}$ ,  $\hat{U}_R^c$ ,  $\hat{D}_R^c$ ,  $\hat{L}$ ,  $\hat{E}_R^c$ ,  $\hat{H}_u$ ,  $\hat{H}_d$  are the superfields for quark doublet, right-handed up-type quark, right-handed down-type quark, lepton doublet, right-handed charged lepton, up-type Higgs doublet, and down-type Higgs doublet, respectively.

Because of the absence of sparticles with mass equal to their SM partners, SUSY has to be broken at a high energy scale in the hidden sector, and then the breaking effects are transmitted to the observable sector. The low energy supersymmetry breaking soft terms

such as gaugino masses, scalar masses, and trilinear soft terms are

$$\begin{aligned}
-\mathcal{L}_{\text{soft}} = & \frac{1}{2} \left( M_3 \tilde{g} \tilde{g} + M_2 \tilde{W} \tilde{W} + M_1 \tilde{B} \tilde{B} \right) \\
& + m_{H_u}^2 |H_u|^2 + m_{H_d}^2 |H_d|^2 + m_S^2 |S|^2 + m_Q^2 |Q|^2 + m_U^2 |U_R|^2 \\
& + m_D^2 |D_R|^2 + m_L^2 |L|^2 + m_E^2 |E_R|^2 \\
& + (h_u A_u Q H_u U_R^c - h_d A_d Q H_d D_R^c - h_e A_e L H_d E_R^c \\
& + \lambda A_\lambda H_u H_d S + \frac{1}{3} \kappa A_\kappa S^3 + h.c.) ,
\end{aligned} \tag{3.2}$$

where  $\tilde{g}$ ,  $\tilde{W}$ , and  $\tilde{B}$  are gluino, Wino, and Bino, respectively.

The NMSSM has five neutralinos ( $\tilde{\chi}_i^0$ ), which are the mass eigenstates of mixings among  $\tilde{B}$ ,  $\tilde{W}$ ,  $\tilde{H}_d^0$ ,  $\tilde{H}_u^0$ , and  $\tilde{S}$ . Following the convention of Ref. [31], we give the mass matrix for the neutralino sector in Appendix A. Because of the extra singlet in the NMSSM, the neutral Higgs sector is also expanded. There are 3 CP-even Higgs ( $H_i$ ) and 2 CP-odd Higgs ( $A_i$ ), both of which are mixed among  $H_d$ ,  $H_u$  and  $S$  gauge eigenstates. We find it is more convenient to discuss the CP-even and CP-odd Higgs mass matrixes in the Goldstone basis [49],  $S_i$ , ( $i = 1, 2, 3$ ) and  $P_i$ , ( $i = 1, 2$ ). Their mass matrixes are presented in Appendix A as well for later discussion.

Now, we are ready to discuss the feasibility of three scenarios that could fulfil the observation of the Galactic Center Gamma-ray Excess in the NMSSM, while agree with the other experimental results. The DM annihilation processes are shown in Fig 1.

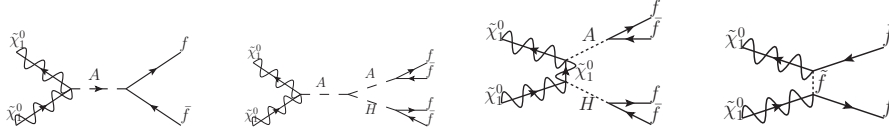


**Figure 1.** The DM annihilation processes in the NMSSM which may explain the GCGE.

### 3.1 s-Channel $A_1$ Resonant Annihilation

As have been studied in Ref. [3], when DM annihilate directly into  $b\bar{b}$ , we need the DM to have mass  $m_{\text{DM}} \sim 35$  GeV and  $\langle\sigma v\rangle|_{v\rightarrow 0} \sim 2 \times 10^{-26}$  cm<sup>3</sup>/s to produce the observed GCGE. Interestingly, the  $b\bar{b}$  final state is commonly favoured due to its relatively larger Yukawa coupling if the  $s$ -channel annihilation is mediated by a relatively light Higgs boson. However, the Higgs boson mediator can not be CP-even mainly because of the following two reasons

- The annihilation which is mediated by  $s$ -channel CP-even Higgs is p-wave suppressed. As have been discussed in Section 2, in this case, the dark matter will annihilate much faster at early time than today. So  $\langle\sigma v\rangle|_{v\rightarrow 0} \sim 2 \times 10^{-26}$  cm<sup>3</sup>/s will lead to very small relic density.
- The CP-even Higgs boson can also mediate the spin independent DM direct detection, from which the bound has been reached as low as  $10^{-9}$  pb [1]. So it is very hard to fulfil the GCGE while satisfy the direct detection constraints.

In principle, the CP-odd Higgs boson can be a very good  $s$ -channel mediator candidate. Firstly, there is no p-wave suppression in its annihilation, which means  $\langle\sigma v\rangle|_{v\rightarrow 0} \sim 2 \times 10^{-26} \text{ cm}^3/\text{s}$  today will just meet the need of getting the right DM relic density. For two fermion with momentum [50]

$$k_1^\mu = (E_1, \vec{k}) = (\sqrt{m_{DM}^2 + \vec{k}^2}, \vec{k}), \quad (3.3)$$

$$k_2^\mu = (E_2, -\vec{k}) = (\sqrt{m_{DM}^2 + \vec{k}^2}, -\vec{k}), \quad (3.4)$$

the spinors can be written as follows

$$u(k_1) = \left( \frac{k_1 \cdot \sigma + m_{DM}}{\sqrt{2(k_1^0 + m_{DM})}} \zeta_1 \quad \frac{k_1 \cdot \bar{\sigma} + m_{DM}}{\sqrt{2(k_1^0 + m_{DM})}} \zeta_1 \right)^T, \quad (3.5)$$

$$v(k_2) = \left( \frac{k_2 \cdot \sigma + m_{DM}}{\sqrt{2(k_2^0 + m_{DM})}} \zeta_2 \quad \frac{k_2 \cdot \bar{\sigma} + m_{DM}}{\sqrt{2(k_2^0 + m_{DM})}} \zeta_2 \right)^T. \quad (3.6)$$

The matrix element of dark matter annihilation with vertex  $\bar{u}\gamma^5 v A$  is

$$\bar{u}\gamma^5 v = -\frac{1}{\sqrt{(E_1 + m_{DM})(E_2 + m_{DM})}} [(E_1 + m_{DM})(E_2 + m_{DM}) + \vec{k}^2] (\zeta_1^\dagger \zeta_2), \quad (3.7)$$

which is  $s$ -wave dominant, while the p-wave contribution is suppressed by  $\frac{1}{\sqrt{(E_1 + m_{DM})(E_2 + m_{DM})}}$ .

Secondly, the interaction of DM and nucleon through  $t$ -channel CP-odd Higgs is spin dependent. For the same vertex  $\bar{u}\gamma^5 u A$ , the matrix element of direct detection process is

$$\begin{aligned} \bar{u}(p_1)\gamma^5 u(p_2) &= \frac{1}{\sqrt{(p_1^0 + m_{DM})(p_2^0 + m_{DM})}} \xi_1^\dagger [(p_2^0 + m_{DM})(\vec{p}_1 \cdot \vec{\sigma}) - (p_1^0 + m_{DM})(\vec{p}_2 \cdot \vec{\sigma})] \\ &\sim 2(p_1 - p_2)^i (\xi_1^\dagger \hat{S}^i \xi_2), \end{aligned} \quad (3.8)$$

which only gives the spin dependent amplitude. So, the stringent bound from spin independent direct detection does not apply anymore.

However, in the realistic NMSSM, there are more constraints which should be considered. In order to have a relatively large DM annihilation cross section, the CP-odd Higgs boson can not be too heavy. Also, its couplings to the SM particles should be suppressed to evade the current collider searches. Interestingly, a light singlet-like CP-odd Higgs ( $A_1$ ) can just meet the need. As a result, we will assume a light singlet superfield in our model. Also, it is natural to require that our DM be singlino dominant<sup>1</sup>. Its mass is approximately  $m_{\tilde{\chi}_1^0} \sim 2\kappa s$ , which means

$$\frac{\kappa}{\lambda} = \frac{m_{\tilde{\chi}_1^0}}{2\mu_{\text{eff}}} \lesssim \frac{35}{200}, \quad (3.9)$$

---

<sup>1</sup>Ref. [22] showed that DM can also be admixture of Bino and Higgsino. As we will discuss it briefly later, the Bino and Higgsino mixing scenario is similar to the singlino and Higgsino mixing scenario in many aspects.

where the second inequality is from the un-discovered of chargino at the LEP experiment [51]. Also, the condition of no Landau pole up to the GUT scale imposes

$$\sqrt{\lambda^2 + \kappa^2} \lesssim 0.5, \quad (3.10)$$

which indicates that  $\kappa$  can only be  $\lesssim 0.1$ . Besides, the requirement of  $A_1$  being singlet-like suppresses the  $A_1 b\bar{b}$  coupling, although it might be enhanced with relatively large  $\tan\beta$ . So, both vertexes of the process in Fig. 1 are suppressed, and generically it is impossible to get the right relic density as well as the GCGE with such small couplings. However, the resonant enhancement can solve this problem: when the energy of initial states are close to the  $A_1$  mass, the total annihilation cross section is enhanced by a Breit-Wigner factor

$$R(s) = \frac{1}{(s - M_A^2)^2 + \Gamma_A^2 M_A^2}. \quad (3.11)$$

The cross section of such process is given by

$$\langle\sigma v\rangle = \frac{3}{8\pi} \sqrt{1 - \frac{m_b^2}{m_{\tilde{\chi}_1^0}^2}} \frac{\kappa^2 C_{A_1 d} m_b^4 \tan^2 \beta}{(s - m_{A_1}^2)^2 + \Gamma_{A_1}^2 m_{A_1}^2}. \quad (3.12)$$

Thus, we need to require the mass of the CP-odd Higgs  $A_1$  around 70 GeV. But the problem still exists if we want to accommodate the relic density simultaneously. At the early stage of the Universe when DM is freezing out, the temperature of the Universe is around  $m_{\tilde{\chi}_1^0}/20$  [52]. So, the energy of the DM is slightly higher at freezing out than today. And the Breit-Wigner factor is very sensitive to the initial energy around the mediator mass. The  $\langle\sigma v\rangle|_{v\rightarrow 0} \sim 2 \times 10^{-26} \text{ cm}^3/\text{s}$  today will lead to over abundant DM, because of the reduction of resonant enhancement. To increase the annihilation cross section at freezing-out, we may include small Higgsino component in the DM, and then we have additional contribution from the  $s$ -channel  $Z$  boson exchange. From Eqs. (A.7) and (A.8), we need small  $\mu$  to get relatively large Higgsino components in DM. Moreover, the coupling between DM and  $Z$  boson is proportional to  $\tan\beta$ . So, a relatively large  $\tan\beta$  is required in our model as well. As will be shown numerically later, the  $Z\tilde{\chi}_1^0\tilde{\chi}_1^0$  coupling, which can give right DM relic density, is still consistent with the constraint from  $Z$  boson invisible decay. On the contrary, the coupling between the DM and Higgs boson is enhanced by large  $\lambda$ . What's more, the  $\tilde{H}_d$  component in DM is further increased by large  $\tan\beta$ . So,  $h_{\text{SM}}$  may have considerable decay branching ratio to DMs in this scenario.

Following the above argument, we have got the viable DM scenario which can explain the relic density and GCGE, and is consistent with DM direct searches. Before we start the numerical scanning, let us study the parameter space a little bit more to figure out the correlations among the NMSSM parameters.

The singlet tends to be lighter than the SM Higgs boson. Since the measurements of  $h_{\text{SM}}$  are likely to agree with the SM couplings, the mixing between the  $H_u/H_d$  doublets and singlet should be suppressed in most cases. So we can get the approximate value for  $A_\lambda$ , as shown in Eq. (A.11). Also, in the CP-even Higgs matrix, the  $M_A^2$  is enhanced by a factor of  $1/\sin^2 2\beta$ , which will increase greatly with large  $\tan\beta$ . So, we can safely decoupling  $S_1$



component in the CP-even Higgs matrix and  $P_1$  component in the CP-odd Higgs matrix in the following discussions. And then from CP-odd Higgs boson mass matrix in Eq. (A.12), we obtain

$$M_{A_1}^2 \simeq -3A_\kappa \frac{\kappa\mu}{\lambda} + \frac{\lambda^2 v^2}{2\mu} s_{2\beta} (A_\lambda + \frac{4\kappa\mu}{\lambda}) \simeq -3A_\kappa \frac{m_{\tilde{\chi}_1^0}}{2} + \lambda^2 v^2 (1 + \frac{\sin 2\beta m_{\tilde{\chi}_1^0}}{2\mu}) , \quad (3.13)$$

where we have substituted Eq. (A.11) and  $m_{\tilde{\chi}_1^0} \sim 2\kappa s$ . Note that  $m_{\tilde{\chi}_1^0} \sim 35$  GeV,  $\mu \gtrsim 100$  GeV, and  $\tan\beta$  is large, the second term in the bracket of Eq. (3.13) can be ignored. As a result,  $A_\kappa$  is approximately fixed

$$A_\kappa = \frac{2(\lambda^2 v^2 - M_{A_1}^2)}{3m_{\tilde{\chi}_1^0}} . \quad (3.14)$$

Another possible problem is the Higgs invisible decay. Although the direct bound on the SM-like Higgs invisible decay is still very weak,  $\text{Br}(H_{\text{inv}}) \lesssim 75\%$  [53], the current Higgs coupling measurement requires that the Higgs signal strength to the SM particles should be around 1. Since in most of our models, there is no additional Higgs production mechanism, the Higgs invisible decay branching ratio is thus highly constrained indirectly. The main contribution to the vertex  $H_2 \tilde{\chi}_1^0 \tilde{\chi}_1^0$  is the superpotential term  $W = \lambda S H_u H_d$ . And the corresponding coupling for  $H_2 \tilde{\chi}_1^0 \tilde{\chi}_1^0$  is proportional to  $C_{\tilde{\chi}_1^0 d} \frac{\lambda}{\sqrt{2}}$ , where  $C_{\tilde{\chi}_1^0 d}$  is the  $\tilde{H}_d$  component in the DM  $\tilde{\chi}_1^0$ . So we get

$$\Gamma_{H_2 \rightarrow \tilde{\chi}_1^0 \tilde{\chi}_1^0} = \frac{(1/4 m_{H_2}^2 - m_{\tilde{\chi}_1^0}^2)^{\frac{3}{2}}}{\pi m_{H_2}^2} \times \lambda^2 C_{\tilde{\chi}_1^0 d}^2 . \quad (3.15)$$

Thus, the Higgs invisible decay is enhanced by large  $\lambda$  and  $C_{\tilde{\chi}_1^0 d}$ .

Let us summarize the results that we have got so far

- The  $s$ -channel mediator of DM annihilation should be singlet-like CP-odd Higgs boson, whose mass is around  $2 \times m_{\text{DM}}$ . This will fix the  $A_\kappa$  parameter.
- The singlino dominant DM should have small Higgsino component, which requires a small  $\mu$  and large  $\tan\beta$ . Interestingly, natural SUSY only requires a small  $\mu$ .
- The purity of the  $h_{\text{SM}}$  can be fulfilled by setting an appropriate  $A_\lambda$ .
- The Higgs invisible decay should be taken care of seriously.

We use the NMSSMtools [54–56] to survey the viable parameter space in the NMSSM at electroweak scale. While the DM relic density, DM direct and indirect detection rates are calculated by micrOMGAs [57–59]. We apply the following constraints implicitly for the following study

- Theoretical constraints such as the converged RGE running, no tachyon, no Landau pole below the GUT scale, physical global minimal and so on.
- The Higgs and sparticle searches at the LEP and Tevatron experiments.

- $B$  physics constraints.
- $Z$  boson invisible decay width.
- The SM Higgs mass lies in the range of [123, 128] GeV. And its signal strengths for all channels are lies in range of [0.8, 1.2].
- The good dark matter candidate with  $0.09 < \Omega h^2 < 0.12$ ,  $\sigma_{\text{SI}} < 1 \times 10^{-9}$  pb, and  $0.5 \times 10^{-26} \text{cm}^3/\text{s} < \langle \sigma v \rangle < 5 \times 10^{-26} \text{cm}^3/\text{s}$ .

Within the scenario that we have proposed, to further simplify our scanning, we decouple the irrelevant particles by choosing

$$\begin{aligned}
M_1 &= 1 \text{ TeV}, M_2 = 2 \text{ TeV}, M_3 = 3 \text{ TeV}, m_L = m_E = 1 \text{ TeV} , \\
A_e &= 0 \text{ TeV}, m_{Q_2} = 2 \text{ TeV}, m_{Q_3} = 1.5 \text{ TeV}, m_{U_2} = m_{D_2} = 3 \text{ TeV} , \\
m_{U_3} &= 1.5 \text{ TeV}, m_{D_3} = 2.5 \text{ TeV}, A_b = 0 \text{ TeV} .
\end{aligned} \tag{3.16}$$

And we scan the rest of the parameters in the following ranges

$$\begin{aligned}
\lambda &: [0.35, 0.65], \quad \kappa : [30, 45] \times \frac{\lambda}{2\mu}, \quad \tan \beta : [10, 40] , \\
\mu &: [100, 600] \text{ GeV}, \quad A_\kappa : [-100, 100] \text{ GeV} , \\
A_\lambda &= 2\mu/\sin 2\beta - 2\kappa\mu/\lambda, \quad A_t = \mu/\tan \beta + \sqrt{6} \times 1500 .
\end{aligned} \tag{3.17}$$

We present our numerical results in Fig. 2. The DM annihilation today is greatly enhanced by the  $A_1$  resonance, especially in the region  $m_{A_1}/2m_{\tilde{\chi}_1^0} \gtrsim 0.98$ . However, the relic density is relatively large in the resonant region  $m_{A_1}/2m_{\tilde{\chi}_1^0} \rightarrow 1$ . It is mainly because of the reduced Breit-Wigner factor due to the large DM energy at freezing out.

From the upper right panel of Fig. 2, we conclude that the annihilation of DM is still dominated by the  $\kappa$  coupling for  $A_1 \tilde{\chi}_1^0 \tilde{\chi}_1^0$ , even though the  $\kappa$  is preferably more than one order of magnitude smaller than  $\lambda$

$$\lambda C_{\tilde{\chi}_1^0, d} C_{\tilde{\chi}_1^0, d} C_{A_1, s} \ll \kappa C_{\tilde{\chi}_1^0, s}^2 C_{A_1, s} . \tag{3.18}$$

From the figure, we can also find that the coupling between  $A_1$  and bottom quarks is indeed suppressed by its small  $H_d$  component.

On the other hand, the invisible decay of the SM-like Higgs boson  $H_{\text{SM}}$  is dominated by the large  $\lambda$  coupling, as shown in the lower left panel of Fig. 2. Thus, we need the smallness of  $\tilde{H}_d$  component in  $\tilde{\chi}_1^0$  to suppress the coupling between the dark matter and SM-like Higgs boson. Note that because of Eq. (3.9), DM mass will decrease when increasing  $\lambda$ . The smaller Higgs invisible decay branching ratio usually means the heavier dark matter mass.

As we have emphasized before, the Higgsino component in the DM is very important to achieve the correct DM relic density. That is why one usually needs relatively small  $\mu$  and large  $\tan \beta$  in this scenario. As shown in the lower right panel of Fig. 2, we find  $\mu$  preferably lies in the range of [200, 600] GeV, which gives us a handle to discovery this scenario at LHC, by searching for relatively light Higgsinos. We will present more extensive

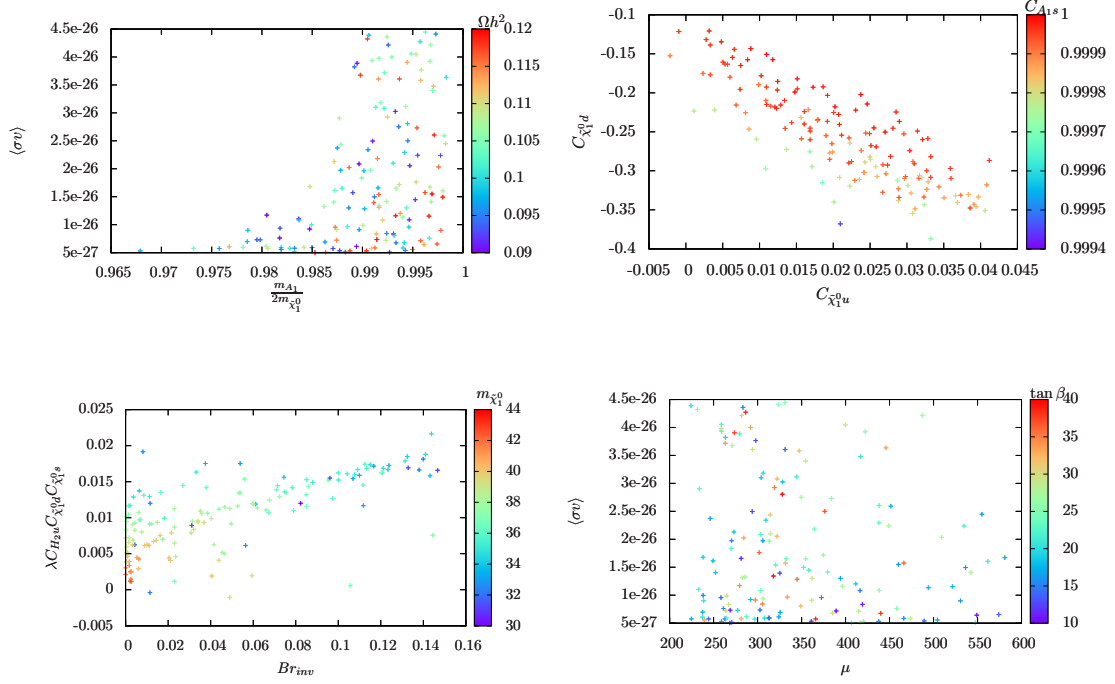


**Figure 2.** All the points in figures satisfy the constraints that mentioned in the Section 3. The corresponding  $x$ -axis and  $y$ -axis as well as colore coding are given in each panel.

study in the next Section. Fig. 3 shows their decay branching ratios, in which both  $\tilde{\chi}_2^0$  and  $\tilde{\chi}_3^0$  have very large decay branching ratios to  $Z\tilde{\chi}_1^0$  and  $H_{SM}\tilde{\chi}_1^0$ . And their decays to lighter Higgs bosons are suppressed by the large singlet component, which usually have branching ratios smaller than 10%.

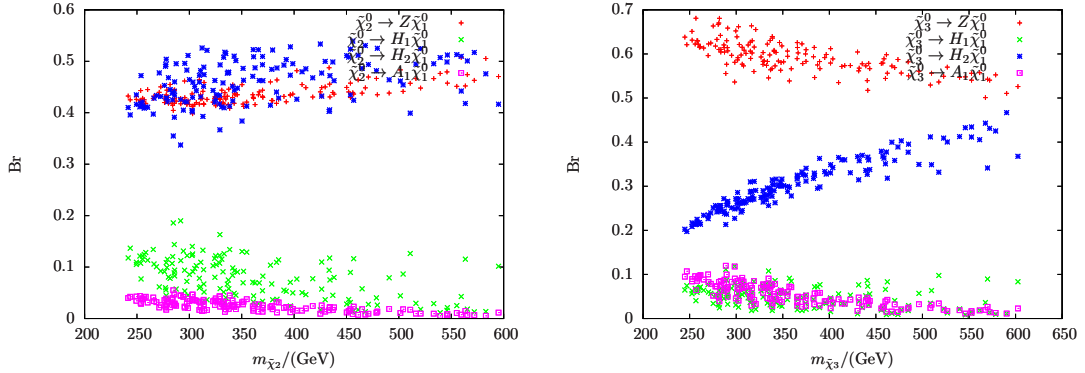


**Figure 3.** All the points in figures satisfy the constraints that mentioned in the Section 3. Left: Decay branching ratios for  $\tilde{\chi}_2^0$ . Right: Decay branching ratios for  $\tilde{\chi}_3^0$ .

In order to have a better understanding of this scenario, we present a benchmark point in Table 1. From this table, the ratios of the DM annihilations into  $b\bar{b}$  and  $e^+e^-$  at freeze

$\lambda$	$\kappa$	$\tan\beta$	$\mu$	$A_\lambda$	$A_\kappa$
0.557	0.033	25.72	313.2	8029.5	9.51
$A_t$	$m_{A_1}$	$m_{H_1}$	$m_{H_2}$	$m_{\tilde{\chi}_1^0}$	$m_{\tilde{\chi}_2^0}$
3686.4	72.1	65.3	124.9	36.4	332.1
$m_{\tilde{\chi}_1^\pm}$	$\frac{\tilde{\chi}_1^0 \tilde{\chi}_1^0 \rightarrow b\bar{b}}{\tilde{\chi}_1^0 \tilde{\chi}_1^0 \rightarrow e^+e^-} \Big _{\text{Freeze Out}}$	$\Omega h^2$	$\langle\sigma v\rangle _{v\rightarrow 0}(\text{cm}^3/\text{s})$	$\sigma_{\text{SI}}(\text{cm}^2)$	$\text{Br}(H_2 \rightarrow \tilde{\chi}_1^0 \tilde{\chi}_1^0)$
319.6	5.5	0.11	$2.25 \times 10^{-26}$	$6.34 \times 10^{-50}$	3.9%
$\text{Br}(\tilde{\chi}_2^0 \rightarrow Z\tilde{\chi}_1^0)$	$\text{Br}(\tilde{\chi}_2^0 \rightarrow H_2\tilde{\chi}_1^0)$	$\text{Br}(\tilde{\chi}_2^0 \rightarrow H_1\tilde{\chi}_1^0)$	$\text{Br}(\tilde{\chi}_3^0 \rightarrow Z\tilde{\chi}_1^0)$	$\text{Br}(\tilde{\chi}_3^0 \rightarrow H_2\tilde{\chi}_1^0)$	$\text{Br}(\tilde{\chi}_3^0 \rightarrow H_1\tilde{\chi}_1^0)$
41.8%	46.3 %	8.8%	59.7%	28.7%	5.4%

**Table 1.** The benchmark point for Scenario 1. which satisfies all the constraints mentioned in the text and whose other soft parameters are given in Eq. (3.16). All mass parameters are in units of GeV.

out are quite similar to the decay branching ratios of  $Z$  boson. So we conclude that the DM annihilations are indeed dominated by the  $Z$  boson exchange in the early Universe, while the  $Z$  boson contributions suffer from both p-wave suppression and away from resonance pole today. For this benchmark point, 90% of the DM annihilations into  $b\bar{b}$ . Following the same analysis as in Ref. [3], we calculate the gamma ray spectrum for this benchmark point by using micrOMEGAs, which is given in Fig. 4. Thus, it can fit the observed GCGE very well.

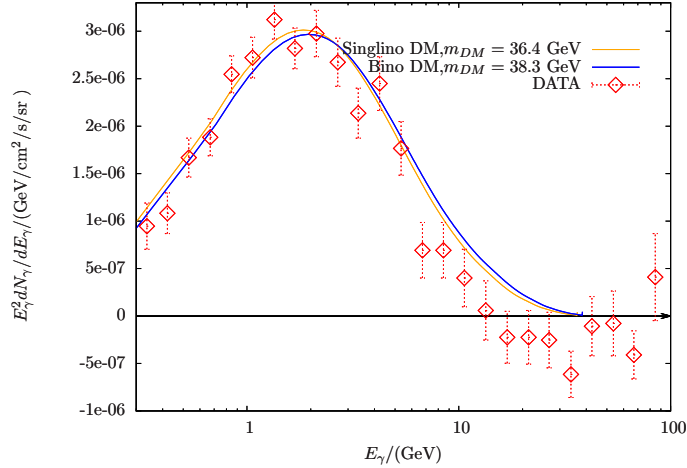


**Figure 4.** The gamma-ray spectra of two benchmark points in Tables 1 and 2. The generalised NFW halo profile with an inner slope of  $\gamma = 1.26$  is chosen. And the angle distance from the Galactic Center is  $5^\circ$ .

Before end up this Section, let us take a brief discussion of the scenario where the DM is Bino dominant. In this case, besides  $\kappa$  becomes a free parameter since there is no constraint on the singlino mass, there is not much difference with the singlino LSP scenario. In order to annihilate Bino DM effectively, we still need the  $A_1$  resonant enhancement. A relatively large Higgsino component is needed to realize the correct DM relic density as well. As a result, except for the singlet state, the rest of the model properties are quite similar with the above singlino LSP scenario. We give a benchmark point in Table 2. For

this benchmark point, because the singlet is heavy, the lightest CP-even Higgs boson is SM-like. And its invisible decay to DM is dominated by gauge coupling. The lightest CP-odd Higgs boson is singlet-like, with its proper mass  $m_{A_1} \sim 2 \times m_{\tilde{\chi}_1^0}$  by tuning  $A_\kappa$ . Moreover, the light Higgsino states decay similarly with the singlino LSP scenario, which are dominated by  $Z\tilde{\chi}_1^0$  and  $H_{\text{SM}}\tilde{\chi}_1^0$  final states.

$\lambda$	$\kappa$	$\tan\beta$	$\mu$	$A_\lambda$	$A_\kappa$
0.173	0.558	30.23	175.5	4220.2	0.56
$A_t$	$m_{A_1}$	$m_{H_1}$	$M_1$	$m_{\tilde{\chi}_1^0}$	$m_{\tilde{\chi}_2^0}$
3234.1	76.75	124.1	41.9	38.3	184.8
$m_{\tilde{\chi}_1^\pm}$	$\Omega h^2$	$\langle\sigma v\rangle _{v\rightarrow 0}(\text{cm}^3/\text{s})$	$\sigma_{\text{SI}}(\text{cm}^2)$	$\text{Br}(H_1 \rightarrow \tilde{\chi}_1^0 \tilde{\chi}_1^0)$	$\text{Br}(A_1 \rightarrow b\bar{b})$
179.7	0.118	$2.38 \times 10^{-26}$	$3.84 \times 10^{-46}$	15%	90%
$\text{Br}(\tilde{\chi}_2^0 \rightarrow Z\tilde{\chi}_1^0)$	$\text{Br}(\tilde{\chi}_2^0 \rightarrow H_1\tilde{\chi}_1^0)$	$\text{Br}(\tilde{\chi}_2^0 \rightarrow A_1\tilde{\chi}_1^0)$	$\text{Br}(\tilde{\chi}_3^0 \rightarrow Z\tilde{\chi}_1^0)$	$\text{Br}(\tilde{\chi}_3^0 \rightarrow H_1\tilde{\chi}_1^0)$	$\text{Br}(\tilde{\chi}_3^0 \rightarrow A_1\tilde{\chi}_1^0)$
52.7%	45.8%	1.5%	90%	8.2%	1.8%

**Table 2.** The benchmark point with Bino-like DM, which satisfies all the constraints mentioned in the text and whose other soft parameters are given in Eq. (3.16). All mass parameters are in units of GeV.

### 3.2 Hidden Sector Dark Matter in the NMSSM

From Ref. [12], there exists another way to explain the GCGE. This solution is called the hidden sector senario from the general NMSSM, where dark matter with mass  $m_{\tilde{\chi}_1^0} \sim 67$  GeV can dominantly annihilate into  $H_1$  and  $A_1$ . Both  $H_1$  and  $A_1$  are singlet-like while having small fractions of  $H_d$  component. And then  $H_1$  and  $A_1$  mainly decay into  $b\bar{b}$  because of the relatively large bottom quark Yukawa coupling. In this Section, we will discuss such scenario in the realistic NMSSM.

The processes of  $\tilde{\chi}_1^0 \tilde{\chi}_1^0 \rightarrow H_1 A_1$  are  $A_1$  mediated  $s$ -channel and  $\tilde{\chi}_i^0$  mediated  $t$ -channel annihilation, as shown in Fig 1. In this case, we can not employ the resonant enhancement because here  $A_1$  should have mass smaller than  $2 \times m_{\text{DM}} - m_{H_1}$ . So, a very large coupling between singlet state is required. As a result, in contrast with previous scenario, Bino can not be a good DM candidate due to its small coupling with Higgs boson. To get a singlino-like dark matter with mass around 67 GeV, we have  $m_\chi \simeq 2\frac{\kappa}{\lambda}\mu$ , which implies

$$\frac{\kappa}{\lambda} = \frac{m_{\tilde{\chi}_1^0}}{2\mu_{\text{eff}}} \lesssim \frac{67}{200}. \quad (3.19)$$

On the other hand, the cross section of dark matter annihilation into  $H_1$  and  $A_1$  is expected to be

$$\langle\sigma v\rangle \simeq \frac{\kappa^4}{4\pi m_{\tilde{\chi}_1^0}^2} \frac{|\vec{P}_3|}{m_{\tilde{\chi}_1^0}} \left( \frac{4m_{\tilde{\chi}_1^0}^2 + m_{A_1}^2 - m_{H_1}^2}{4m_{\tilde{\chi}_1^0}^2 - m_{A_1}^2 - m_{H_1}^2} - \frac{m_{\tilde{\chi}_1^0}^2 - A_\kappa m_{\tilde{\chi}_1^0}}{4m_{\tilde{\chi}_1^0}^2 - m_{A_1}^2} \right)^2, \quad (3.20)$$

in which  $|\vec{P}_3| = \sqrt{E_{A_1}^2 - m_{A_1}^2}$ , and  $E_{A_1} = \sqrt{\frac{4m_\chi^2 + m_{A_1}^2 - m_{H_1}^2}{4m_\chi}}$ . We find  $\langle\sigma v\rangle$  can be affected by  $\kappa$ ,  $m_{A_1}$ , and  $m_{H_1}$ : the later two mainly affect the phase space through  $\frac{|\vec{P}_3|}{m_{\tilde{\chi}_1^0}}$  while  $\kappa$

will affect the cross section through  $\kappa^4$ . As we shall see numerically later, in the NMSSM, there is a tension between the  $\kappa$  and  $|\vec{P}_3|$  which prevents us from getting relatively large DM annihilation cross section. Also, a larger  $\kappa$ , which is required from large  $\langle\sigma v\rangle$ , may result in a larger  $m_{H_1}$  and  $m_{A_1}$ , which gives a smaller  $\frac{|\vec{P}_3|}{m_{\tilde{\chi}_1^0}}$ .

The dark matter direct detection experiments also give strong constraint on DM-nucleon scattering cross section. The recent LUX results show for  $m_{DM} \simeq 50$  GeV,  $\sigma_{SI} < 1 \times 10^{-9}$  pb. In our case, for a singlino dominant dark matter, the main contributions to direct detection come from  $H_1$  and  $H_2$  mediated  $t$ -channel processes. The spin independent DM-nucleon cross section is

$$\sigma_{SI} \simeq \frac{\kappa^2 \mu_{\tilde{\chi}_1^0 N}^2 m_N^2 f_N^2}{4\pi v^2} \left( \frac{C_{H1u}}{m_{H_1}^2} + \frac{C_{H2s}}{m_{H_2}^2} \right)^2, \quad (3.21)$$

where  $f_N = \sum_{q=u,d,s} f_{T_q} + \frac{2}{9} f_{T_G} \simeq 0.348 \pm 0.015$  [60],  $C_{H1u}$  and  $C_{H2s}$  are the  $H_u$  component in  $H_1$  and singlet component in  $H_2$ , respectively. To get a small  $\sigma_{SI}$ , it is necessary to have a quite small mixing between  $H_u^0$  and  $S$  due to

$$C_{H1u}^2 \simeq \sigma_{SI} \frac{4\pi v^2 m_{H_1}^4}{0.1^2 f_N^2} \left( \frac{0.1}{\kappa} \right)^2 < 0.004. \quad (3.22)$$

And to suppress the singlet component in the SM-like  $H_2$ , we use the condition  $A_\lambda = 2\mu/\sin 2\beta - 2\kappa\mu/\lambda$ . Moreover, from Eq. (3.19) and Landau pole condition  $\lambda^2 + \kappa^2 \lesssim 0.5$ , we have

$$|\kappa| \lesssim \sqrt{\frac{1}{2} \left( \frac{m_{\tilde{\chi}_1^0}^2}{m_{\tilde{\chi}_1^0}^2 + 4\mu^2} \right)}. \quad (3.23)$$

In order to have a relatively large  $\kappa \gtrsim 0.1$  which is required by Eq. (3.20),  $\mu$  can only have value  $\lesssim 200$  GeV. And then the DM can have relatively large Higgsino component because of the incomplete cancellation of the off-diagonal term. So the spin independent DM-nucleon scattering cross section is further enhanced. As we will show numerically later, it is very difficult to achieve the very large DM annihilation cross section, while escape the DM direct detection constraints.

Follow the same strategy as above, we survey the parameter space in the low energy NMSSM. We choose the same irrelevant soft terms as Eq. (3.16), and the ranges for the DM related parameters as follows

$$\begin{aligned} \lambda &: [0.35, 0.65], \quad \kappa : -[50, 100] \times \frac{\lambda}{2\mu}, \quad \tan \beta : [1, 40] \\ \mu &: [100, 500] \text{ GeV}, \quad A_\kappa : [-100, 100] \text{ GeV} \\ A_\lambda &= 2\mu/\sin 2\beta - 2\kappa\mu/\lambda, \quad A_t = \mu/\tan \beta + \sqrt{6} \times 1500, \end{aligned} \quad (3.24)$$

where a negative  $\kappa$  is taken to reduce the SM-like Higgs invisible decay into  $A_1 A_1$ .

From Fig. 5, to have a suitable dark matter mass without the Landau pole problem,  $\mu$  is dominantly in the range of  $[100, 200]$  GeV, and the relatively large  $|\kappa| (\gtrsim 0.1)$  only appears

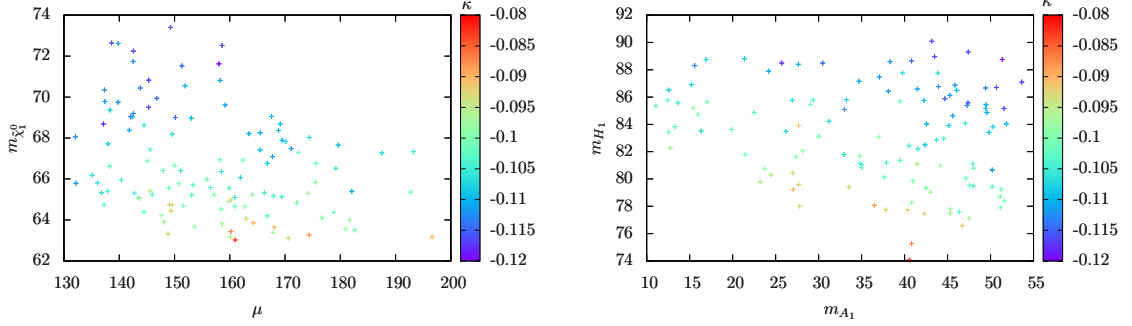


**Figure 5.** All the points in plots satisfy the constraints that mentioned in Section 3. Left: The input parameter  $\mu$  versus  $m_{\tilde{\chi}_1^0}$ , and color shows the value of  $\kappa$ . Right: The lightest CP-odd Higgs boson mass versus the lightest CP-even Higgs boson mass, and the color gives the corresponding value of  $\kappa$  parameter.

at very small  $\mu (\lesssim 160 \text{ GeV})$ . Moreover, we find that  $\kappa$  plays a key role in controlling the  $H_1$  and  $A_1$  masses. A larger  $\kappa$  tends to have both heavier  $H_1$  and  $A_1$ . As a result,  $|\kappa|$  can not be too large in order to have the accessible phase space of DM annihilation into  $H_1$  and  $A_1$ .

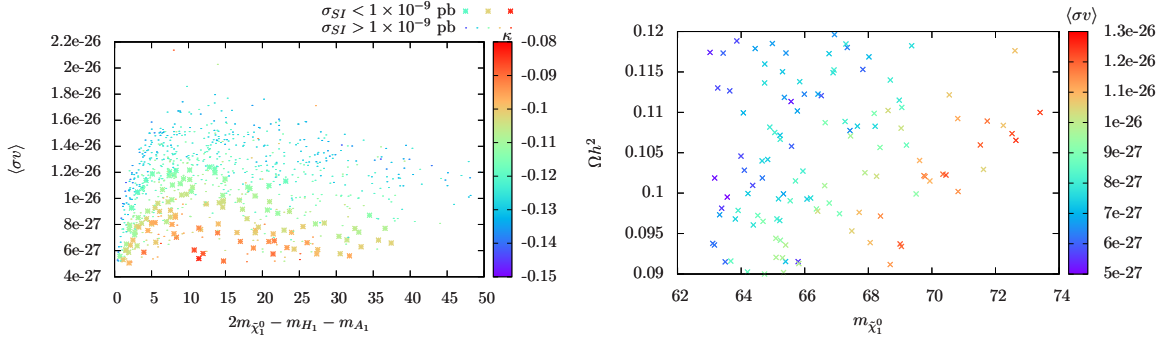


**Figure 6.** Left: The recent direct detection LUX experiment gives a strong constraint. Because the larger  $\kappa$  means larger  $\sigma_{SI}$ , it is difficult to get a big  $\langle\sigma v\rangle$ , and  $\langle\sigma v\rangle > 1.5 \times 10^{-26} \text{ cm}^3/\text{s}$  has been excluded by the LUX results. Right: All the points satisfy the constraints mentioned in the last two figures, so we can find an upper limit on  $\langle\sigma v\rangle$ .

However, there is another more stringent constraint from DM direct detection experiment such as LUX. As have been discussed above, the spin-independent DM-nucleon scattering cross section is also proportional to  $\kappa^2$ . Thus, the large  $\kappa$ , which is required by the GCGE, is highly in conflict with the direct detection. As shown in the left panel of Fig. 6, the LUX experiment constrains  $|\kappa|$  to be no larger than 0.12. This will lead to the DM annihilation cross section smaller than  $\sim 1.2 \times 10^{-26} \text{ cm}^3/\text{s}$ . On the other hand, because of the less degree of freedom for scalar final state, we need  $|\kappa| \gtrsim 0.15$  to reach the

observed gamma ray excess. From the right panel of the figure, we conclude that there is no great tension between the DM density and DM annihilation rate. However, a heavier DM tends to have a relatively large annihilation rate because of large  $|\kappa|$ . In short, the GCGE in this scenario is constrained by Landau pole condition and DM direct search. And it is very difficult to have the DM annihilation cross section as large as expected,  $2.2 \times 10^{-26} \text{cm}^3/s$ .

We present a benchmark point for this scenario in Table 3. This case usually has very small  $\mu$  and relatively large  $|\kappa|$ . The spin-independent DM-nucleon cross section is close to the exclusion limit, while the annihilation cross section only reaches  $1.22 \times 10^{-26} \text{cm}^3/s$ .

$\lambda$	$\kappa$	$\tan\beta$	$\mu$	$A_\lambda$	$A_\kappa$
0.374	-0.113	26.09	143.82	3846.26	39.716
$A_t$	$m_{A_1}$	$m_{H_1}$	$m_{H_2}$	$m_{\tilde{\chi}_1^0}$	$m_{\tilde{\chi}_2^0}$
3679.7	43.9	86.9	125.9	70.43	153.3
$m_{\tilde{\chi}_1^\pm}$	$\Omega h^2$	$\langle\sigma v\rangle _{v\rightarrow 0}(\text{cm}^3/s)$	$\sigma_{\text{SI}}(\text{cm}^2)$	$\text{Br}(H_2 \rightarrow A_1 A_1)$	$\text{Br}(H_1 \rightarrow b\bar{b})$
147.3	0.1026	$1.22 \times 10^{-26}$	$9.43 \times 10^{-46}$	4.5%	89.6%
$\text{Br}(\tilde{\chi}_2^0 \rightarrow Z\tilde{\chi}_1^0)$	$\text{Br}(\tilde{\chi}_2^0 \rightarrow H_2\tilde{\chi}_1^0)$	$\text{Br}(\tilde{\chi}_2^0 \rightarrow A_1\tilde{\chi}_1^0)$	$\text{Br}(\tilde{\chi}_3^0 \rightarrow Z\tilde{\chi}_1^0)$	$\text{Br}(\tilde{\chi}_3^0 \rightarrow H_2\tilde{\chi}_1^0)$	$\text{Br}(\tilde{\chi}_3^0 \rightarrow H_1\tilde{\chi}_1^0)$
0%	0 %	96.3%	62.3%	0%	29.96%

**Table 3.** The benchmark point for Scenario 2. which satisfies all the constraints mentioned in the text. Also, the other soft parameters are given in Eq. (3.16). All mass parameters are in units of GeV.

### 3.3 Sbottom and Stau Coannihilation

If a sparticle has mass very close to the DM, the coannihilation [61] between the sparticle and DM at the early Universe can be very effective. This effect can lead to a DM density agree with the measured value. Moreover, the existence of a very light sbottom or stau may generate the GCGE through the process in Fig. 1. In this Section, we discuss the sbottom and stau coannihilation scenarios confronting with the GCGE briefly.

A light sbottom is constrained by many experiments. Firstly, the precise measurement of  $Z$  boson decay width leads to

$$\Delta\Gamma_Z < 4.7\text{MeV} . \quad (3.25)$$

The coupling of  $Z\tilde{b}_1\tilde{\bar{b}}_1$ , which is

$$C_{Z\tilde{b}_1\tilde{\bar{b}}_1} = -\frac{1}{2}\sin^2\theta_b + \frac{1}{3}\sin^2\theta_W , \quad (3.26)$$

can be reduced by choosing appropriate mixing angle ( $\theta_b \sim \pm 0.4$ ) between two sbottom mass eigenstates. Secondly, the coupling between the light sbottom and Higgs should be suppressed as well. Because it can lead to additional decay mode of Higgs ( $H_{\text{SM}} \rightarrow \tilde{b}_1\tilde{\bar{b}}_1$ ) and may enhance the  $\gamma\gamma$  signal strength. Ref. [62] has found that indeed there is a parameter space with both suppressed  $C_{Z\tilde{b}_1\tilde{\bar{b}}_1}$  and  $C_{H_{\text{SM}}\tilde{b}_1\tilde{\bar{b}}_1}$  couplings. For a light bottom with mass  $m_{\tilde{b}_1} \sim 35$  GeV, the mixing angle  $\theta_b$  can range from 0.02 to 0.6, depending on the heavier



sbottom mass  $m_{\tilde{b}_2}$ . What's more, a light sbottom is constrained directly by the LHC SUSY searches. However, the searches are either rely on high multiplicity of energetic jets or large missing transverse energy ( $E_T^{\text{miss}}$ ). Because there is no energetic jet in the sbottom decay for co-annihilation scenario, the detection of this scenario should be based on a hard Initial State Radiation (ISR), which may produce the relatively large  $E_T^{\text{miss}}$  by recoiling the sbottom to the ISR jet. However, the hardness of the ISR jet is depending on the sbottom mass [63]. For a light sbottom, the hard ISR events is quite rare even its production cross section is relatively large. The light stau is having similar argument as above for its coupling with  $Z$  boson and Higgs boson. And its direct LHC search bound is much looser than sbottom because of its much smaller production rate.

Now, we can turn to the dark matter properties in these scenarios. Since we have  $m_{\tilde{b}_1} \simeq m_{\tilde{\chi}_1^0}$  for sbottom coannihilation scenario, the DM annihilation is dominated by the sbottom mediated  $t$ -channel process. If we assume the coupling of vertex  $\tilde{b}_1 b \tilde{\chi}_1^0$  is  $aP_L + bP_R$ , the annihilation cross section  $\tilde{\chi}_1 \tilde{\chi}_1 \rightarrow b\bar{b}$  will be

$$\langle\sigma v\rangle = \frac{3}{16\pi} \frac{[(a^2 + b^2)m_{\tilde{\chi}_1} + 2abm_b]^2}{(m_{\tilde{\chi}_1}^2 + m_b^2)^2}. \quad (3.27)$$

For  $m_{\tilde{\chi}_1^0} \simeq m_{\tilde{b}_1} \simeq 35$  GeV, to have the cross section for the observed GCGE

$$\langle\sigma v\rangle = 2 \times 10^{-26} \text{ cm}^3/s = 6.67 \times 10^{-37} \text{ cm}^2 \simeq 1.3 \times 10^{-9} \text{ GeV}^{-2}, \quad (3.28)$$

we need either  $a^4$  or  $b^4 \simeq 1.4 \times 10^{-4}$ . On the other hand, the spin-independent cross section mediated by the sbottom is expected to be:

$$\sigma_{SI} = \frac{m_{\tilde{\tau}}^2 m_p^2 f_{TG}^2 a^2 b^2}{729\pi m_b^2 ((m_{\tilde{\chi}_1} + m_b)^2 - m_{\tilde{b}_1}^2)^2}. \quad (3.29)$$

The cross section is greatly enhanced in the region with  $m_{\tilde{b}_1} \simeq m_{\tilde{\chi}_1^0}$ . As a result, for the sbottom co-annihilation models with required GCGE, the spin independent cross section is usually as large as  $\sim 10^{-6}$  pb, which is obviously excluded by the LUX experiment.

In the stau coannihilation scenario, the final states of DM annihilation will be  $\tau$  leptons. The analysis in Ref. [3] shows that the DM in this case should have mass  $\sim 10$  GeV to have a good fit with Fermi-LAT data, which means the lighter stau  $\tilde{\tau}_1$  should have mass around 10 GeV as well. However, as have been studied in Ref. [18], the constraint on  $Z$  boson invisible decay width ( $\Delta\Gamma_{\text{inv}}(Z) < 2.0$  MeV) excludes  $\tilde{\tau}$  lighter than  $\sim 38$  GeV in the stau coannihilation scenario. So, we can not realize the required gamma ray excess in this scenario as well.

## 4 Discovery Potential at the LHC

From previous study, we show that the Scenario 1 with singlino dominant DM is more promising, and then we will only study its dicoverly potential at the LHC. As we know, there are mainly two remarkable signatures of the viable NMSSM with GCGE. The first one is that the DM particle has relatively large Higgsino component and moderately large

coupling to the  $Z$  boson which guarantee the correct DM relic density. So, a natural thought will be the direct production of DM pair at LHC through  $s$ -channel  $Z$  boson exchange. The second signature is the existence of a relatively light Higgsino together with  $\sim 35$  GeV DM, whose dominate decay modes are

$$\tilde{H}^\pm \rightarrow W^\pm \tilde{\chi}_1^0, \quad (4.1)$$

$$\tilde{H}_{1,2}^0 \rightarrow Z \tilde{\chi}_1^0 / H \tilde{\chi}_1^0. \quad (4.2)$$

The decay branching ratios are given in Fig. 3. We shall discuss each signature in details in the following.

#### 4.1 Dark Matter Production Versus Mono-jet

If only one DM pair is produced at hadron collider, it will not leave any information inside the detector. One way to probe this process is through an hard ISR jet, which is recoiling against the DM pair. As result, the signal presents a large in-balanced transverse energy. At the LHC, the CMS Collaboration has carried out the mono-jet search [64] with data set of  $20 \text{ fb}^{-1}$ . Their analysis shows that the current stage of LHC is only sensitive to signals with  $p_T(\text{ISR}) > 280, 340, 450 \text{ GeV}$  that have cross section greater than about 100, 30, 10 fb, respectively.

As for our signal process, even though the direct production is relatively large ( $\sim 10$  pb) because of the small DM mass. The production rate of the signal mono-jet is quite low based on the following reason. As have been studied in Ref. [63], the spectrum of the radiated jet mainly depends on the mass scale of the final states. In our case, because the DM mass is very small ( $\sim 35 \text{ GeV}$ ), the production of an energetic ISR jet is suppressed. From the left panel of Fig. 7, we conclude that the  $p_T$  spectrum of the ISR jet drops very quickly and only  $\sim 1/10^{-4}$  fraction of the events have  $p_T(\text{ISR}) > 250 \text{ GeV}$ . And the situation will not get much better if the LHC goes to the next stage. We show the cross section for the allowed models with different cuts on the leading ISR jet and the corresponding CMS exclusion bounds in the right panel of Fig. 7.

The production cross section drops by about four orders of magnitude after we require the leading ISR to have  $p_T > 280 \text{ GeV}$ . So the signal is around two orders of magnitude smaller than the current bound. And the sensitivity will not become better for harder cuts on the leading ISR jet, *i.e.*, different signal region. So, we may conclude that it will be very difficult to probe the GCGE NMSSM through mono-jet signature at the LHC, even at 14 TeV.

#### 4.2 Searching the Di-Higgs Final State

The detection of the Higgs boson pair production is not only important for discovery of new physics but also important for testing the SM itself. As a signature in our models, the Higgs particles can be pair produced by the neutral Higgsino pair production, which subsequently decay into Higgs and DM with large branching ratios as shown in Fig. 3.

At the LHC, the neutral Higgsino pair is mainly produce through  $s$ -channel  $Z$  boson exchange. As a result, the production cross section is dominated by the coupling between

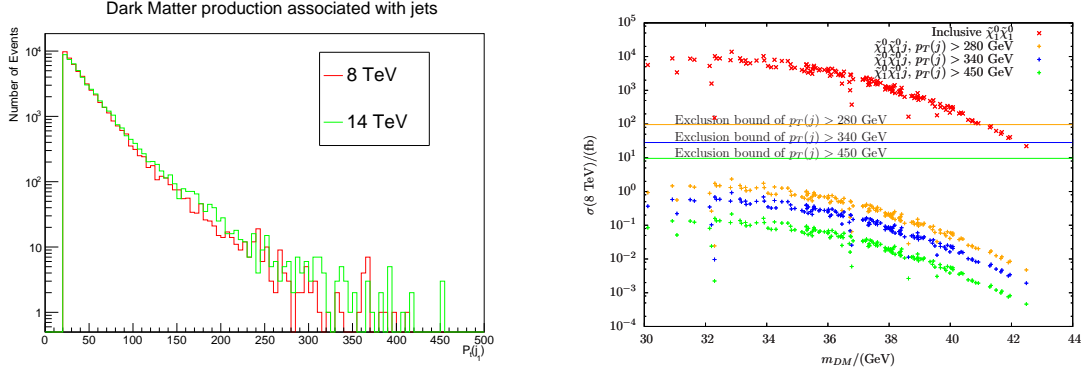


**Figure 7.** Left: the  $p_T$  spectrum of the leading ISR jet for 35.5 GeV DM pair production at LHC. Right: the cross section in the models for the CGGE with corresponding cuts on the leading ISR jet as indicated in the figure. The horizontal lines are the experimental bounds on cross sections for three categories of the models.

the  $Z$  boson and Higgsino pair

$$Z_\mu \tilde{\chi}_i^0 \tilde{\chi}_j^0 = \frac{ie}{2s_W c_W} \gamma^\mu ((Z_{i4}^* Z_{j4}^* - Z_{i3}^* Z_{j3}^*) P_L + (Z_{j4}^* Z_{i4}^* - Z_{j3}^* Z_{i3}^*) P_R), \quad (4.3)$$

where  $N_{ij}$  is the neutralino mixing matrix. We show the mixing factor  $(Z_{i4}^* Z_{j4}^* - Z_{i3}^* Z_{j3}^*)$  for the different combinations in the left panel of Fig. 8. From this figure, we know that in our case, the dominant production of neutral Higgsino pair is  $\tilde{\chi}_2^0 \tilde{\chi}_3^0$ , *i.e.*, the one with different masses.

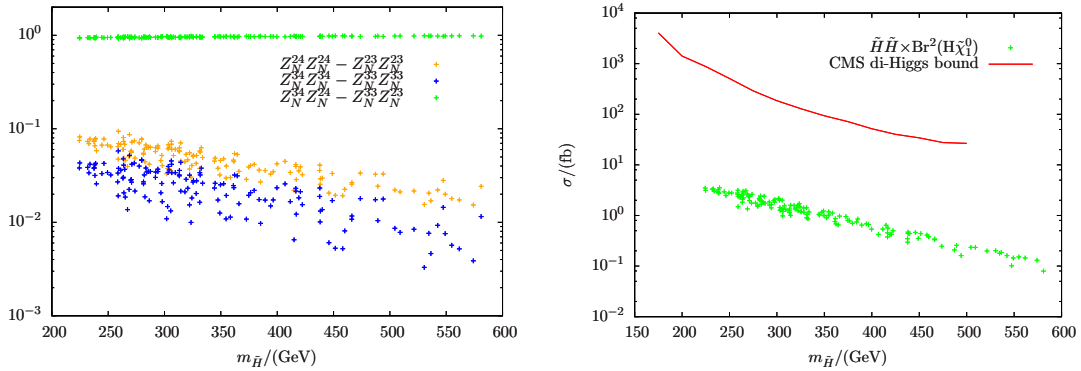


**Figure 8.** Left: the mixing factor of  $Z$  coupling to each pair of neutral Higgsinos. Right: the cross section for the signal models and exclusion bound by the CMS Collaboration.

In Ref. [65], the CMS Collaboration has also tried to search for the di-Higgs signal from Higgsino decay. Because of the slightly excess in the observed number of event, very loose bound is obtained as shown by the red line in the right panel of Fig. 8. The green points in the same figure show the corresponding cross sections of our signal processes. Our models are far beyond the reach for the di-Higgs analysis based on the current data base.

### 4.3 Extrapolating the ATLAS Electroweakino Searches at 14 TeV LHC

In this subsection, we will study two traditional but much more sensitive channels

$$\tilde{\chi}_{2,3}^0 \tilde{\chi}_1^\pm \rightarrow H_{\text{SM}} \tilde{\chi}_1^0 + W^\pm \tilde{\chi}_1^0, \quad (4.4)$$

$$\tilde{\chi}_{2,3}^0 \tilde{\chi}_1^\pm \rightarrow Z \tilde{\chi}_1^0 + W^\pm \tilde{\chi}_1^0. \quad (4.5)$$

In fact, these two channels also give rise to the most stringent bounds on Winos at 8 TeV LHC searches. For  $WH$  final states [66], the Wino mass has been excluded up to  $\sim 300$  GeV for  $m_{\tilde{\chi}_1^0} \sim 35$  GeV. And for  $WZ$  final states [67], all Wino mass below 420 GeV for  $m_{\tilde{\chi}_1^0} \sim 35$  GeV are excluded. As in our case, the production rates of the chargino and neutralino pairs are suppressed due to the mixing between Higgsino states. Moreover, the required final states are suppressed by their decay branching ratio. Thus, in order to get some sensitivities to the NMSSM model with GCGE, we have to consider the 14 TeV LHC.

#### 4.3.1 $WH$ Final States

The ATLAS analysis in Ref. [66], where  $W$  boson decays leptonically while the Higgs boson decays to  $b\bar{b}$ , gives the strongest bound for this channel. Because this search has similar interesting neutralino and chargino mass regions with ours, we will follow their analysis at 8 TeV and try to extrapolate to 14 TeV with minor changes. The cuts are chosen as below

- Exactly one lepton with  $p_T > 25$  GeV.
- There should be no more than 3 jets in the event.
- The leading two jets should be  $b$ -tagged. And their invariant mass is in the range [105,135] GeV. Furthermore, the contranverse mass of the two  $b$ -jets

$$m_{CT}^2 = (E_T^{b1} + E_T^{b2})^2 - |\mathbf{p}_T^{b1} - \mathbf{p}_T^{b2}|^2 \quad (4.6)$$

is larger than 160 GeV.

- To remove the  $W + jets$  background, the transverse mass of the lepton and missing transverse momentum

$$m_T = \sqrt{2p_T^{\text{lep}} E_T^{\text{miss}} - 2\mathbf{p}_T^{\text{lep}} \cdot \mathbf{p}_T^{\text{miss}}} \quad (4.7)$$

is required to be larger than 130 GeV since our Higgsinos tend to be heavier than 200 GeV.

- We define two signal regions SRA and SRB for different masses of Higgsino which correspond to  $E_T^{\text{miss}} > 100$  and  $E_T^{\text{miss}} > 245$ , respectively. We find that the SRB is more sensitive for Higgsino mass greater than 300 GeV.

The dominant backgrounds for our analyses are  $t\bar{t}$ , single top, and  $Wb\bar{b}$ . We generate those backgrounds by MadGraph5 [68], where Pythia6 [69] and Delphes 3.1.2 [70] have been packed to implement parton shower and detector simulation. The  $t\bar{t}$  is generated

up to two additional jets, where the MLM matching adopted in MadGraph5 is used to avoid double counting between matrix element and parton shower. All three single top production modes ( $t$ -channel,  $s$ -channel and  $tW$  process) are considered in our generation. And we use the default ATLAS setup for detector simulation. Their cross sections before and after the cuts for both signal regions are shown in Table 4.

	$\sigma(14 \text{ TeV})/\text{pb}$	SRA/fb	SRB/fb
$t\bar{t}$	877.2	0.39	$2.3 \times 10^{-2}$
single top	318.5	0.064	$3.2 \times 10^{-3}$
$Wb\bar{b}$	128	0.0096	$6.4 \times 10^{-4}$

**Table 4.** The background cross sections before and after the cuts for each signal region.

As for the cut efficiency of signal processes  $\epsilon_s$ , because we have DM mass  $\sim 35$  GeV and Higgsino mass in the range  $[200, 600]$  GeV, we generate the process of  $\tilde{\chi}_2^0 \tilde{\chi}_1^\pm$  pair production with subsequent decays  $\tilde{\chi}_1^\pm \rightarrow W^\pm \tilde{\chi}_1^0$  and  $\tilde{\chi}_2^0 \rightarrow H_{\text{SM}} \tilde{\chi}_1^0$  in Madgraph5 as well. The step size for Higgsino mass is chosen as 20 GeV.

After getting the cut efficiency for the signal events, we can roughly estimate the exclusion bound according to

$$\sigma \sim \frac{S}{\sqrt{B}} = \frac{\sigma_s \epsilon_s}{\sigma_b \epsilon_b} \times \mathcal{L}, \quad (4.8)$$

where  $\sigma_b \epsilon_b$  is given in Table 4 and  $\mathcal{L}$  is luminosity. The corresponding 3- $\sigma$  exclusion limit for the  $WH$  final states is shown as red curve in the left panel of Fig. 9.

The production cross section of the signal process for each of our NMSSM model is calculated by feeding the SLHA [71] output which is generated from NMSSMtools to Madgraph5. And we assume a K-factor of 1.2 for all those models. After we have get those cross sections of the signal process, we project our models to the exclusion plane which we have obtained before. The results are given in Fig. 9. From which we conclude that a large amount of our models can be detected at 14 TeV LHC with luminosity  $5000 \text{ fb}^{-1}$ .

#### 4.3.2 $WZ$ Final States

The searches for both 3-lepton final states [45] and 2-lepton + jets [67] give very strong bound on this decay modes of chargino and neutralino pair productions. And the current bound is actually given by the combination of these two searches. Even though the tri-lepton search is more sensitive for lighter chargino and neutralino region, the 2-lepton + jets are slightly better at higher mass region. Thus, in this subsection, we will re-produce the SR-Zjets analysis in Ref. [67] and extrapolate it to 14 TeV LHC. The cuts chosen by ATLAS Collaboration are listed as follows

- Exact two opposite same sign flavor (OSSF) leptons are required. Also, these two leptons should have  $p_T(l_1) > 35$  GeV and  $p_T(l_2) > 20$  GeV, respectively.
- Because the OSSF lepton pair is decaying from a moderately boosted  $Z$  boson, two additional cuts on leptons are imposed:  $81.2 \text{ GeV} < m_{ll} < 101.2 \text{ GeV}$ ,  $p_T(ll) > 80$

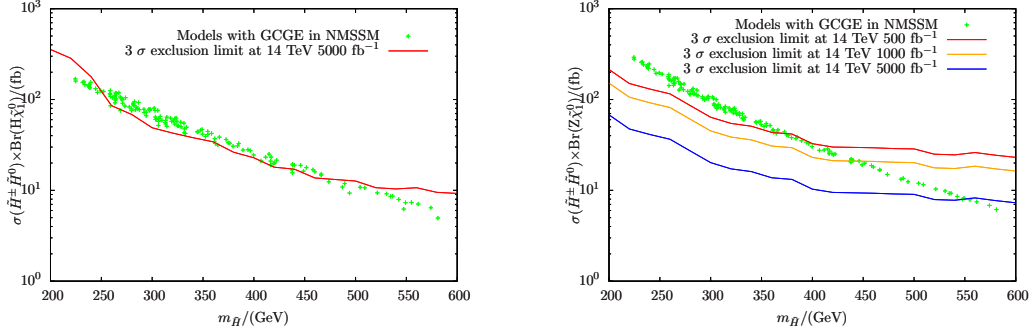


**Figure 9.** Left: the production cross section of  $WH$  final states and its corresponding exclusion limit at 14 TeV LHC with luminosity  $5000 \text{ fb}^{-1}$ . Right: the production cross sections of  $WZ$  final states and their corresponding exclusion limits at 14 TeV LHC with luminosities  $500 \text{ fb}^{-1}$ ,  $1000 \text{ fb}^{-1}$  and  $5000 \text{ fb}^{-1}$ , respectively.

GeV. In addition, the angular separation between two leptons must satisfy  $0.3 < \Delta R(l\bar{l}) < 1.5$ .

- There should be no  $b$ -jet,  $\tau$ -jet and forward jet in the event.
- The two highest- $p_T$  central jets must have  $p_T > 45 \text{ GeV}$ . They are expected from  $W$  boson decay and then satisfy the invariant mass range  $50 \text{ GeV} < m_{jj} < 100 \text{ GeV}$ .
- A cut on  $E_T^{\text{miss,rel}}$  is applied:  $E_T^{\text{miss,rel}} > 80 \text{ GeV}$ , where

$$E_T^{\text{miss,rel}} = \begin{cases} E_T^{\text{miss}} & , \text{ if } \Delta\phi_{l,j} \geq \pi/2 \\ E_T^{\text{miss}} \times \Delta\phi_{l,j} & , \text{ if } \Delta\phi_{l,j} < \pi/2 \end{cases} \quad (4.9)$$

where  $\Delta\phi$  is the azimuthal angle between the direction of  $\mathbf{p}_T^{\text{miss}}$  and that of the nearest lepton or jet.

The dominant backgrounds are leptonic decay of  $W^\pm W^\mp$ , leptonic decay of  $W^\pm Z$  where the lepton from  $W$  decay is not reconstructed, and  $ZZ$  with one of the  $Z$  boson decay into charged leptons while the other decay into neutrinos. All of those backgrounds are generated with up to two additional jets by Madgraph5 with procedure similar to the above. In this case, the cross section before and after the cuts are given in Table 5.

	$\sigma(14 \text{ TeV})/\text{pb}$	SR/fb
$W^\pm W^\mp + \text{jets}$	124.3	0.029
$W^+ Z + \text{jets}$	31.5	0.028
$W^- Z + \text{jets}$	20.32	0.012
$ZZ + \text{jets}$	17.72	0.13

**Table 5.** The background cross sections before and after the cuts for  $WZ$  final states.

As have been done for the  $WH$  process, the signal process for  $WZ$  final states is generated similarly. And the expected 3- $\sigma$  exclusion limits for 14 TeV LHC with luminosities

500 fb<sup>-1</sup>, 1000 fb<sup>-1</sup>, and 5000 fb<sup>-1</sup> are given in the right panel of Fig. 9. From the figure, we can find the sensitivity for  $WZ$  channel is much better than  $WH$  channel, especially at low mass region of Higgsino. At 14 TeV 500 fb<sup>-1</sup> LHC, the NMSSM models with Higgsino lighter than  $\sim 370$  GeV may be excluded.

## 5 Conclusion

We have discussed three possible scenarios in the NMSSM with discrete  $Z_3$  symmetry, which may be able to explain the GCGE. The first scenario,  $s$ -channel  $A_1$  resonant annihilation into  $b\bar{b}$ , is the most promising scenario to realize the gamma-ray excess. In this scenario, even though the GCGE is produced by the  $A_1$  resonant annihilation, the DM annihilation at freezing-out is mainly contributed from the  $s$ -channel  $Z$  boson exchange process. In order to get the correct DM relic density, the coupling between  $Z$  boson and DM is enhanced by relatively large Higgsino component in the DM and large  $\tan\beta$ . The second one is called hidden sector dark matter scenario, in which DM is annihilating into singlet Higgs pair. The subsequent decays of these Higgs bosons into  $b$  quark are able to produce the observed GCGE. However, In the NMSSM, the DM mass, the DM coupling with Higgs bosons, and Higgsino mass are highly correlated. And we do need relatively large singlino dominant DM  $\sim 76$  GeV and larger superpotential coupling  $\kappa$  to implement the GCGE. As a result, the DM annihilation cross section is bounded from above by DM direct detection. So, the GCGE are only mildly fitted. We also briefly discussed the third scenario for the sbottom and stau coannihilations. Even though the existence of very light sbottom and stau are still allowed according to current data, they are not able to explain the observed GCGE because of the constraints from the DM direct detection LUX experiment and  $Z$  boson invisible decay width, respectively.

Because the first scenario is promising, we studied its LHC phenomenology of the viable NMSSM models with GCGE. The discovery potential of four signatures are discussed in details. First, the DM pair production which recoils against a hard ISR jet. Because the energy spectrum of the ISR jet is suppressed by the small DM mass, the production rate of the required signal event is two orders of magnitude smaller than current sensitivity. And such situation will not become better even for the next phase of LHC. Second, the pair production of neutral Higgsinos, which subsequently decay into Higgs pair. This channel, despite of its interesting feature, is two orders of magnitude smaller than current sensitivity as well. Two traditional channels are the chargino and neutralino pair productions which decay into  $WH$ +DMs and  $WZ$ +DMs, respectively. By extrapolating two most sensitive analyses by the ATLAS Collaboration, we found that most of the NMSSM model space is discoverable at 14 TeV LHC with luminosity 5000 fb<sup>-1</sup> for  $WH$  final states while only requires 500 fb<sup>-1</sup> for  $WZ$  channel.

**Note:** When we finalized this paper, there was a new paper [72] on arXiv which studies the similar signature in the MSSM as in our subsection 4.3. But the mass region is a little bit different.

## Acknowledgements

We would like to thank Yandong Liu very much for collaboration at the early stage of the work. This research was supported in part by the Australian Research Council through Grant No. CE110001004 (CoEPP) and by the University of Adelaide (JL and AGW), as well as by the Natural Science Foundation of China under grant numbers 10821504, 11075194, 11135003, 11275246, and 11475238, and by the National Basic Research Program of China (973 Program) under grant number 2010CB833000 (JG and TL).

## A Neutralino and Higgs Mass Matrices

We use the convention in Ref. [31]

$$\tan\beta = \frac{v_u}{v_d}, \quad (\text{A.1})$$

$$\mu_{\text{eff}} = \lambda v_s, \quad (\text{A.2})$$

$$M_A^2 = \frac{2\lambda v_s}{\sin 2\beta} (A_\lambda + \kappa v_s), \quad (\text{A.3})$$

$$v = \sqrt{v_u^2 + v_d^2} = 174 \text{ GeV}, \quad (\text{A.4})$$

where  $v_d$ ,  $v_u$ , and  $s$  are the vacuum expectation values (VEVs) of  $H_d$ ,  $H_u$ , and  $S$ , respectively. The symmetric neutralino mass matrix in the  $(\tilde{B}, \tilde{W}, \tilde{H}_d, \tilde{H}_u, \tilde{S})$  basis can be written as follows

$$\mathcal{M}_0 = \begin{pmatrix} M_1 & 0 & -\frac{g_1 v_d}{\sqrt{2}} & \frac{g_1 v_u}{\sqrt{2}} & 0 \\ & M_2 & \frac{g_2 v_d}{\sqrt{2}} & -\frac{g_2 v_u}{\sqrt{2}} & 0 \\ & & 0 & -\mu_{\text{eff}} & -\lambda v_u \\ & & & 0 & -\lambda v_d \\ & & & & 2\kappa s \end{pmatrix}. \quad (\text{A.5})$$

The lightest neutralino is the mixing of gauge eigenstates

$$\tilde{\chi}_1^0 = N_{11}\tilde{B} + N_{12}\tilde{W} + N_{13}\tilde{H}_u + N_{14}\tilde{H}_d + N_{15}\tilde{S}, \quad (\text{A.6})$$

and its mass approximately is  $m_{\tilde{\chi}_1^0} \sim 2\kappa s$  if it is singlino-like. In the  $2\kappa/\lambda \ll 1$  limit, the Higgsino components of the  $\tilde{\chi}_1^0$  can be estimated as below [22]

$$\frac{N_{13}}{N_{15}} = \frac{\lambda v}{\mu^2 - m_{\tilde{\chi}_1^0}^2} c_\beta (t_\beta m_{\tilde{\chi}_1^0} - \mu), \quad (\text{A.7})$$

$$\frac{N_{14}}{N_{15}} = \frac{-\lambda v}{\mu^2 - m_{\tilde{\chi}_1^0}^2} s_\beta \left( \mu - \frac{m_{\tilde{\chi}_1^0}}{t_\beta} \right), \quad (\text{A.8})$$

where we have used  $c_\beta$ ,  $s_\beta$ , and  $t_\beta$  for  $\cos\beta$ ,  $\sin\beta$ , and  $\tan\beta$ , respectively.

The  $3 \times 3$  symmetric CP-even Higgs boson mass matrix in the  $(S_1, S_2, S_3)$  basis [49] is

$$\mathcal{M}_S^2 = \begin{pmatrix} M_A^2 + s_{2\beta}^2(m_Z^2 - \lambda^2 v^2) & s_{2\beta}c_{2\beta}(m_Z^2 - \lambda^2 v^2) & -\lambda v c_{2\beta}(A_\lambda + \frac{2\kappa\mu}{\lambda}) \\ c_{2\beta}^2 m_Z^2 + \lambda^2 v^2 s_{2\beta}^2 & 2\lambda v(\mu - s_\beta c_\beta(A_\lambda + \frac{2\kappa\mu}{\lambda})) & \frac{s_{2\beta}}{2} \frac{\lambda^2 v^2}{\mu} A_\lambda + \frac{\kappa\mu}{\lambda}(A_\kappa + 4\frac{\kappa\mu}{\lambda}) \end{pmatrix}. \quad (\text{A.9})$$



In the case of very light singlet, the singlet component of the SM Higgs  $H_{\text{SM}}$  can be suppressed by requiring

$$(\mathcal{M}_S^2)_{23} \simeq 0. \quad (\text{A.10})$$

The Eq. (A.10) can be used to determine the approximation value of  $A_\lambda$  as follows

$$A_\lambda \simeq \frac{2\mu}{s_{2\beta}} - \frac{2\kappa\mu}{\lambda}. \quad (\text{A.11})$$

At last, we give the simplest  $2 \times 2$  symmetric CP-odd Higgs mass matrix in the  $(P_1, P_2)$  basis

$$\mathcal{M}_P^2 = \begin{pmatrix} M_A^2 & \lambda v(A_\lambda - 2\frac{\kappa\mu}{\lambda}) \\ -\frac{3\kappa\mu A_\kappa}{\lambda} + \frac{\lambda^2 v^2}{2\mu} s_{2\beta}(A_\lambda + \frac{4\kappa\mu}{\lambda}) & \end{pmatrix}. \quad (\text{A.12})$$

## References

- [1] **LUX Collaboration** Collaboration, D. Akerib *et al.*, “First results from the LUX dark matter experiment at the Sanford Underground Research Facility,” *Phys.Rev.Lett.* **112** (2014) 091303, [1310.8214](#).
- [2] **SuperCDMS Collaboration** Collaboration, R. Agnese *et al.*, “Search for Low-Mass WIMPs with SuperCDMS,” *Phys.Rev.Lett.* **112** (2014) 241302, [1402.7137](#).
- [3] T. Daylan, D. P. Finkbeiner, D. Hooper, T. Linden, S. K. N. Portillo, *et al.*, “The Characterization of the Gamma-Ray Signal from the Central Milky Way: A Compelling Case for Annihilating Dark Matter,” [1402.6703](#).
- [4] A. Alves, S. Profumo, F. S. Queiroz, and W. Shepherd, “The Effective Hooperon,” [1403.5027](#).
- [5] A. Berlin, D. Hooper, and S. D. McDermott, “Simplified Dark Matter Models for the Galactic Center Gamma-Ray Excess,” *Phys.Rev.* **D89** (2014) 115022, [1404.0022](#).
- [6] P. Agrawal, B. Batell, D. Hooper, and T. Lin, “Flavored Dark Matter and the Galactic Center Gamma-Ray Excess,” [1404.1373](#).
- [7] E. Izaguirre, G. Krnjaic, and B. Shuve, “The Galactic Center Excess from the Bottom Up,” *Phys.Rev.* **D90** (2014) 055002, [1404.2018](#).
- [8] S. Ipek, D. McKeen, and A. E. Nelson, “A Renormalizable Model for the Galactic Center Gamma Ray Excess from Dark Matter Annihilation,” [1404.3716](#).
- [9] P. Ko, W.-I. Park, and Y. Tang, “Higgs portal vector dark matter for GeV scale  $\gamma$ -ray excess from galactic center,” [1404.5257](#).
- [10] M. Abdullah, A. DiFranzo, A. Rajaraman, T. M. Tait, P. Tanedo, *et al.*, “Hidden On-Shell Mediators for the Galactic Center Gamma-Ray Excess,” *Phys.Rev.* **D90** (2014) 035004, [1404.6528](#).
- [11] A. Martin, J. Shelton, and J. Unwin, “Fitting the Galactic Center Gamma-Ray Excess with Cascade Annihilations,” [1405.0272](#).
- [12] A. Berlin, P. Gratia, D. Hooper, and S. D. McDermott, “Hidden Sector Dark Matter Models for the Galactic Center Gamma-Ray Excess,” *Phys.Rev.* **D90** (2014) 015032, [1405.5204](#).

- [13] J. M. Cline, G. Dupuis, Z. Liu, and W. Xue, “The windows for kinetically mixed  $Z'$ -mediated dark matter and the galactic center gamma ray excess,” *JHEP* **1408** (2014) 131, [1405.7691](#).
- [14] D. K. Ghosh, S. Mondal, and I. Saha, “Confronting the Galactic Center Gamma Ray Excess With a Light Scalar Dark Matter,” [1405.0206](#).
- [15] C. Boehm, M. J. Dolan, and C. McCabe, “A weighty interpretation of the Galactic Centre excess,” *Phys.Rev.* **D90** (2014) 023531, [1404.4977](#).
- [16] L. Wang, “A simplified 2HDM with a scalar dark matter and the galactic center gamma-ray excess,” [1406.3598](#).
- [17] P. Agrawal, M. Blanke, and K. Gemmler, “Flavored dark matter beyond Minimal Flavor Violation,” [1405.6709](#).
- [18] T. Han, Z. Liu, and S. Su, “Light Neutralino Dark Matter: Direct/Indirect Detection and Collider Searches,” *JHEP* **1408** (2014) 093, [1406.1181](#).
- [19] J. Huang, T. Liu, L.-T. Wang, and F. Yu, “Supersymmetric Sub-Electroweak Scale Dark Matter, the Galactic Center Gamma-ray Excess, and Exotic Decays of the 125 GeV Higgs Boson,” [1407.0038](#).
- [20] C. Balz and T. Li, “Simplified Dark Matter Models Confront the Gamma Ray Excess,” [1407.0174](#).
- [21] B. D. Fields, S. L. Shapiro, and J. Shelton, “Galactic Center Gamma-Ray Excess from Dark Matter Annihilation: Is There A Black Hole Spike?,” [1406.4856](#).
- [22] C. Cheung, M. Papucci, D. Sanford, N. R. Shah, and K. M. Zurek, “NMSSM Interpretation of the Galactic Center Excess,” [1406.6372](#).
- [23] K. Kong and J.-C. Park, “Bounds on Dark Matter Interpretation of Fermi-LAT GeV Excess,” [1404.3741](#).
- [24] T. Bringmann, M. Vollmann, and C. Weniger, “Updated cosmic-ray and radio constraints on light dark matter: Implications for the GeV gamma-ray excess at the Galactic center,” [1406.6027](#).
- [25] M. Cirelli, D. Gaggero, G. Giesen, M. Taoso, and A. Urbano, “Antiproton constraints on the GeV gamma-ray excess: a comprehensive analysis,” [1407.2173](#).
- [26] N. Okada and O. Seto, “Galactic center gamma ray excess from two Higgs doublet portal dark matter,” [1408.2583](#).
- [27] D. Borah and A. Dasgupta, “Galactic Center Gamma Ray Excess in a Radiative Neutrino Mass Model,” [1409.1406](#).
- [28] M. Cahill-Rowley, J. Gainer, J. Hewett, and T. Rizzo, “Towards a Supersymmetric Description of the Fermi Galactic Center Excess,” [1409.1573](#).
- [29] **ATLAS Collaboration** Collaboration, G. Aad *et al.*, “Observation of a new particle in the search for the Standard Model Higgs boson with the ATLAS detector at the LHC,” *Phys.Lett.* **B716** (2012) 1–29, [1207.7214](#).
- [30] **CMS Collaboration** Collaboration, S. Chatrchyan *et al.*, “Observation of a new boson at a mass of 125 GeV with the CMS experiment at the LHC,” *Phys.Lett.* **B716** (2012) 30–61, [1207.7235](#).
- [31] U. Ellwanger, C. Hugonie, and A. M. Teixeira, “The Next-to-Minimal Supersymmetric Standard Model,” *Phys.Rept.* **496** (2010) 1–77, [0910.1785](#).

- [32] U. Ellwanger, G. Espitalier-Noel, and C. Hugonie, “Naturalness and Fine Tuning in the NMSSM: Implications of Early LHC Results,” *JHEP* **1109** (2011) 105, [1107.2472](#).
- [33] G. G. Ross and K. Schmidt-Hoberg, “The Fine-Tuning of the Generalised NMSSM,” *Nucl.Phys.* **B862** (2012) 710–719, [1108.1284](#).
- [34] L. J. Hall, D. Pinner, and J. T. Ruderman, “A Natural SUSY Higgs Near 126 GeV,” *JHEP* **1204** (2012) 131, [1112.2703](#).
- [35] Z. Kang, J. Li, and T. Li, “On Naturalness of the MSSM and NMSSM,” *JHEP* **1211** (2012) 024, [1201.5305](#).
- [36] J.-J. Cao, Z.-X. Heng, J. M. Yang, Y.-M. Zhang, and J.-Y. Zhu, “A SM-like Higgs near 125 GeV in low energy SUSY: a comparative study for MSSM and NMSSM,” *JHEP* **1203** (2012) 086, [1202.5821](#).
- [37] J. Cao, Z. Heng, J. M. Yang, and J. Zhu, “Status of low energy SUSY models confronted with the LHC 125 GeV Higgs data,” *JHEP* **1210** (2012) 079, [1207.3698](#).
- [38] J. R. Espinosa, C. Grojean, V. Sanz, and M. Trott, “NSUSY fits,” *JHEP* **1212** (2012) 077, [1207.7355](#).
- [39] M. Perelstein and B. Shakya, “XENON100 implications for naturalness in the MSSM, NMSSM, and lambda-supersymmetry model,” *Phys.Rev.* **D88** (2013), no. 7, 075003, [1208.0833](#).
- [40] K. Agashe, Y. Cui, and R. Franceschini, “Natural Islands for a 125 GeV Higgs in the scale-invariant NMSSM,” *JHEP* **1302** (2013) 031, [1209.2115](#).
- [41] S. King, M. Muhlleitner, and R. Nevzorov, “NMSSM Higgs Benchmarks Near 125 GeV,” *Nucl.Phys.* **B860** (2012) 207–244, [1201.2671](#).
- [42] S. King, M. Mhilleitner, R. Nevzorov, and K. Walz, “Natural NMSSM Higgs Bosons,” *Nucl.Phys.* **B870** (2013) 323–352, [1211.5074](#).
- [43] **CMS Collaboration** Collaboration, V. Khachatryan *et al.*, “Observation of the diphoton decay of the Higgs boson and measurement of its properties,” [1407.0558](#).
- [44] **ATLAS Collaboration** Collaboration, G. Aad *et al.*, “Measurement of Higgs boson production in the diphoton decay channel in  $pp$  collisions at center-of-mass energies of 7 and 8 TeV with the ATLAS detector,” [1408.7084](#).
- [45] **ATLAS Collaboration** Collaboration, G. Aad *et al.*, “Search for direct production of charginos and neutralinos in events with three leptons and missing transverse momentum in  $\sqrt{s} = 8\text{TeV}$   $pp$  collisions with the ATLAS detector,” *JHEP* **1404** (2014) 169, [1402.7029](#).
- [46] J. F. Navarro, A. Ludlow, V. Springel, J. Wang, M. Vogelsberger, *et al.*, “The Diversity and Similarity of Cold Dark Matter Halos,” [0810.1522](#).
- [47] J. Diemand, M. Kuhlen, P. Madau, M. Zemp, B. Moore, *et al.*, “Clumps and streams in the local dark matter distribution,” *Nature* **454** (2008) 735–738, [0805.1244](#).
- [48] **Planck Collaboration** Collaboration, P. Ade *et al.*, “Planck 2013 results. XVI. Cosmological parameters,” *Astron.Astrophys.* (2014) [1303.5076](#).
- [49] D. Miller, R. Nevzorov, and P. Zerwas, “The Higgs sector of the next-to-minimal supersymmetric standard model,” *Nucl.Phys.* **B681** (2004) 3–30, [hep-ph/0304049](#).
- [50] J. Kumar and D. Marfatia, “Matrix element analyses of dark matter scattering and annihilation,” *Phys.Rev.* **D88** (2013), no. 1, 014035, [1305.1611](#).

- [51] “[http://lepsusy.web.cern.ch/lepsusy/www/inoslowdmsummer02/charginolowdm\\_pub.html](http://lepsusy.web.cern.ch/lepsusy/www/inoslowdmsummer02/charginolowdm_pub.html),”.
- [52] G. Jungman, M. Kamionkowski, and K. Griest, “Supersymmetric dark matter,” *Phys.Rept.* **267** (1996) 195–373, [hep-ph/9506380](#).
- [53] **ATLAS Collaboration** Collaboration, G. Aad *et al.*, “Search for Invisible Decays of a Higgs Boson Produced in Association with a Z Boson in ATLAS,” *Phys.Rev.Lett.* **112** (2014) 201802, [1402.3244](#).
- [54] U. Ellwanger, J. F. Gunion, and C. Hugonie, “NMHDECAY: A Fortran code for the Higgs masses, couplings and decay widths in the NMSSM,” *JHEP* **0502** (2005) 066, [hep-ph/0406215](#).
- [55] U. Ellwanger and C. Hugonie, “NMHDECAY 2.0: An Updated program for sparticle masses, Higgs masses, couplings and decay widths in the NMSSM,” *Comput.Phys.Commun.* **175** (2006) 290–303, [hep-ph/0508022](#).
- [56] G. Belanger, F. Boudjema, C. Hugonie, A. Pukhov, and A. Semenov, “Relic density of dark matter in the NMSSM,” *JCAP* **0509** (2005) 001, [hep-ph/0505142](#).
- [57] G. Belanger, F. Boudjema, A. Pukhov, and A. Semenov, “micrOMEGAs\_3: A program for calculating dark matter observables,” *Comput.Phys.Commun.* **185** (2014) 960–985, [1305.0237](#).
- [58] G. Belanger, F. Boudjema, P. Brun, A. Pukhov, S. Rosier-Lees, *et al.*, “Indirect search for dark matter with micrOMEGAs2.4,” *Comput.Phys.Commun.* **182** (2011) 842–856, [1004.1092](#).
- [59] G. Belanger, F. Boudjema, A. Pukhov, and A. Semenov, “Dark matter direct detection rate in a generic model with micrOMEGAs 2.2,” *Comput.Phys.Commun.* **180** (2009) 747–767, [0803.2360](#).
- [60] J. M. Cline, K. Kainulainen, P. Scott, and C. Weniger, “Update on scalar singlet dark matter,” *Phys.Rev.* **D88** (2013) 055025, [1306.4710](#).
- [61] K. Griest and D. Seckel, “Three exceptions in the calculation of relic abundances,” *Phys.Rev.* **D43** (1991) 3191–3203.
- [62] B. Batell, C. E. M. Wagner, and L.-T. Wang, “Constraints on a Very Light Sbottom,” *JHEP* **1405** (2014) 002, [1312.2590](#).
- [63] J. Alwall, S. de Visscher, and F. Maltoni, “QCD radiation in the production of heavy colored particles at the LHC,” *JHEP* **0902** (2009) 017, [0810.5350](#).
- [64] **ATLAS Collaboration** Collaboration, G. Aad *et al.*, “Search for pair-produced third-generation squarks decaying via charm quarks or in compressed supersymmetric scenarios in  $pp$  collisions at  $\sqrt{s}=8$  TeV with the ATLAS detector,” [1407.0608](#).
- [65] **CMS Collaboration** Collaboration, C. Collaboration, “Search for electroweak production of higgsinos in channels with two Higgs bosons decaying to b quarks in  $pp$  collisions at 8 TeV,”.
- [66] T. A. collaboration, “Search for chargino and neutralino production in final states with one lepton, two b-jets consistent with a Higgs boson, and missing transverse momentum with the ATLAS detector in  $20.3 \text{ fb}^{-1}$  of  $\sqrt{s} = 8$  TeV  $pp$  collisions,”.
- [67] **ATLAS Collaboration** Collaboration, G. Aad *et al.*, “Search for direct production of charginos, neutralinos and sleptons in final states with two leptons and missing transverse

momentum in  $pp$  collisions at  $\sqrt{s} = 8$  TeV with the ATLAS detector,” *JHEP* **1405** (2014) 071, [1403.5294](#).

- [68] J. Alwall, M. Herquet, F. Maltoni, O. Mattelaer, and T. Stelzer, “MadGraph 5 : Going Beyond,” *JHEP* **1106** (2011) 128, [1106.0522](#).
- [69] T. Sjostrand, S. Mrenna, and P. Z. Skands, “PYTHIA 6.4 Physics and Manual,” *JHEP* **0605** (2006) 026, [hep-ph/0603175](#).
- [70] **DELPHES 3** Collaboration, J. de Favereau *et al.*, “DELPHES 3, A modular framework for fast simulation of a generic collider experiment,” *JHEP* **1402** (2014) 057, [1307.6346](#).
- [71] B. Allanach, C. Balazs, G. Belanger, M. Bernhardt, F. Boudjema, *et al.*, “SUSY Les Houches Accord 2,” *Comput.Phys.Commun.* **180** (2009) 8–25, [0801.0045](#).
- [72] C. Han, “Probing light bino and higgsinos at the LHC,” [1409.7000](#).